Publications

6-2016

The White Dwarf Luminosity Function

Enrique Garcia-Berro
Universitat Politecnica de Catalunya

Terry D. Oswalt
Embry-Riddle Aeronautical University, oswaltt1@erau.edu

Follow this and additional works at: https://commons.erau.edu/publication

Scholarly Commons Citation

The white dwarf luminosity function

Enrique García–Berro[a,b], Terry D. Oswalt[c]

[a]*Departament de Física, Universitat Politècnica de Catalunya, c/Esteve Terrades 5, 08860 Castelldefels, Spain*
[b]*Institut d'Estudis Espacials de Catalunya, c/Gran Capità 2–4, Edif. Nexus 104, 08034 Barcelona, Spain*
[c]*Department of Physical Sciences, Embry-Riddle Aeronautical University, 600 Clyde Morris Boulevard, Daytona Beach, FL 32114*

Abstract

White dwarfs are the final remnants of low- and intermediate-mass stars. Their evolution is essentially a cooling process that lasts for ~ 10 Gyr. Their observed properties provide information about the history of the Galaxy, its dark matter content and a host of other interesting astrophysical problems. Examples of these include an independent determination of the past history of the local star formation rate, identification of the objects responsible for the reported microlensing events, constraints on the rate of change of the gravitational constant, and upper limits to the mass of weakly interacting massive particles. To carry on these tasks the essential observational tools are the luminosity and mass functions of white dwarfs, whereas the theoretical tools are the evolutionary sequences of white dwarf progenitors, and the corresponding white dwarf cooling sequences. In particular, the observed white dwarf luminosity function is the key manifestation of the white dwarf cooling theory, although other relevant ingredients are needed to compare theory and observations. In this review we summarize the recent attempts to empirically determine the white dwarf luminosity function for the different Galactic populations. We also discuss the biases that may affect its interpretation. Finally, we elaborate on the theoretical ingredients needed to model the white dwarf luminosity function, paying special attention to the remaining uncertainties, and we comment on some applications of the white dwarf cooling theory. Astrophysical problems for which white dwarf stars

Email addresses: `enrique.garcia-berro@upc.edu` (Enrique García–Berro), `terry.oswalt@erau.edu` (Terry D. Oswalt)

may provide useful leverage in the near future are also discussed.

1. Introduction

White dwarfs are the final evolutionary stage of stars with masses less than $10\pm2\,M_\odot$, though the upper mass limit is not yet well known (Ritossa et al., 1999). Van Dyk et al. (2003), Smartt et al. (2004), Maund et al. (2005) and Li et al. (2006) attempted to provide observational limits on the maximum progenitor mass. Most white dwarfs are composed of carbon and oxygen, but those with masses less than $0.4\,M_\odot$ are made of helium, while those more massive than $\sim 1.05\,M_\odot$ are made of oxygen and neon (Garcia-Berro and Iben, 1994). The exact composition of the carbon-oxygen core critically depends on the processes occuring during the previous Asymptotic Giant Branch (AGB) phase. Theoretical calculations show that the precise ratio of carbon to oxygen depends, to a large extent, on the competition between the ^{12}C$(\alpha,\gamma)^{16}$O and the triple-α reactions (Salaris et al., 1997), on the particular details of the stellar evolutionary codes used to compute the pre-white dwarf evolutionary phases (Renedo et al., 2010), on the adopted convective prescription and on the choice of several other physical inputs (Althaus et al., 2005b). In a typical white dwarf of $0.58\,M_\odot$, oxygen represents 62% of the total mass, while its concentration in the central layers of the white dwarf can be as high as 85% (Wood, 1992; Salaris et al., 1997). In all cases, the core is surrounded by a thin layer of pure helium with a mass ranging from 10^{-2} to $10^{-4}\,M_\odot$. Masses larger than $10^{-2}\,M_\odot$ are not possible, as this would lead to helium ignition at the base of the shell. This region is, in turn, surrounded by an even thinner layer of hydrogen with mass within the range 10^{-4} to $10^{-15}\,M_\odot$. This layer is missing in $\sim 20\%$ of white dwarfs, and determines the basic chemical composition of their envelopes.

From a phenomenological point of view, white dwarfs with hydrogen spectral lines are classified as DA. The rest are classified as DO, DB, DQ, DZ and DC, depending on their spectral features, roughly constituting a sequence of decreasing temperatures (Sion et al., 1983), and have helium-dominated atmospheres. It is well established that white dwarfs with helium-rich atmospheres are the result of a late shell flash, and that the subsequent evolution results in distinct atmospheric features. For instance, a dredge-up episode

2

is at the origin of DQ white dwarfs, while DZ white dwarfs are the result of external pollution by metals. DO and DB white dwarfs have surface layers which are made of almost pure helium, only differing in effective temperature, which determines the corresponding spectral features, while DC white dwarfs are characterized by the absence of helium spectral lines at low temperatures. Although our basic understanding of the physical mechanisms that lead to the formation of the different white dwarf spectral types is on solid grounds, several details still need to be studied, as there is an interplay between the mechanisms operating in the envelopes of white dwarfs, such as gravitational settling, thermal diffusion, radiative levitation, convection at the H-He and He-core interfaces, proton burning, stellar winds and mass accretion from the interstellar medium. These interesting topics are, however, out of the scope of our paper — a good summary can be found in Chen and Hansen (2012). Most of the observational efforts to empirically determine the white dwarf luminosity function have been done employing samples of DA white dwarfs. For this reason we will focus primarily on work done on these types of white dwarfs.

White dwarfs have rather simple mechanical structures. In fact, their stability is mostly provided by the pressure of degenerate electrons and to remain in hydrostatic equilibrium — that is, to balance gravity with the pressure gradient — the energy release of thermonuclear reactions is not needed. Because of this, their evolution can be described as a simple cooling process (Mestel, 1952) in which the internal degenerate core acts as a reservoir of energy and the outer non-degenerate layers modulate the energy outflow. In the simplest picture it is assumed that the core is isothermal, which is justified by the high conductivity of degenerate electrons and the thin envelope. Under these conditions energy conservation may be written as:

$$L \approx -\frac{dU}{dt} = -\langle c_{\mathrm{V}} \rangle M_{\mathrm{WD}} \frac{dT_{\mathrm{c}}}{dt} \qquad (1)$$

where U is the thermal content, $\langle c_{\mathrm{V}} \rangle$ is the average specific heat, T_{c} is the temperature of the nearly isothermal core, and M_{WD} is the mass of the white dwarf. Additionally, the luminosity of the star and the temperature of the isothermal core are, to first order, related through the expression:

$$L = f(T_{\mathrm{c}}) M_{\mathrm{WD}} \qquad (2)$$

where $f(T_{\mathrm{c}})$ is a function which depends on the detailed thermal structure of the envelope. This set of equations can be integrated, provided that $f(T_{\mathrm{c}})$ is

given. A simple calculation indicates that the cooling timescales of these stars are very long, ~ 10 Gyr, and thus the white dwarf population largely remains visible throughout the cooling process and retains important information about the past history of the Galaxy.

In particular, this allows us to derive useful constraints on the stellar formation rate (Noh and Scalo, 1990; Diaz-Pinto et al., 1994; Isern et al., 1995, 2001) and the age (Winget et al., 1987; Garcia-Berro et al., 1988; Wood, 1992; Hernanz et al., 1994; Oswalt et al., 1996; Bergeron et al., 1997; Richer et al., 2000, 2006) of the different Galactic components: disk, halo as well as open clusters and globular clusters. Moreover, it has been conjectured that those white dwarfs that are not detectable could contribute substantially to the dark matter content of our Galaxy. Specifically, surveys carried out by the MACHO team Alcock et al. (1995, 1997, 2000) suggested that a substantial fraction of the halo dark matter could be in the form of very cool white dwarfs. Since then, the EROS (Lasserre et al., 2000; Goldman et al., 2002; Tisserand et al., 2007), OGLE (Udalski et al., 1996), MOA (Muraki et al., 1999) and SuperMACHO (Becker et al., 2005) teams have monitored millions of stars during several years in both the Large Magellanic Cloud (LMC) and the Small Magellanic Cloud (SMC) to search for microlensing events. Most of them have challenged the results of the MACHO experiment — see, for instance, Yoo et al. (2004) and references therein. In addition, there have been several claims that white dwarfs could be the stellar objects reported in the Hubble Deep Field (Ibata et al., 1999; Méndez and Minniti, 2000; Kilic et al., 2005). However, these claims remain inconclusive for lack of spectroscopic identifications and confirmed proper motions. The Hubble Deep Field–South has provided another opportunity to test the contribution of white dwarfs to the Galactic dark matter content. In particular, three white dwarf candidates among several faint blue objects which exhibit significant proper motion have been found (Kilic et al., 2005). They are assumed to belong to the thick disk or halo populations. If these are spectroscopically confirmed, it would imply that white dwarfs account for $\lesssim 10\%$ of the Galactic dark matter, which would fit comfortably within the results of the EROS team. All in all, the study of the white dwarf population has important ramifications for our understanding of the structure and evolution of the Milky Way.

The fundamental tool for studying the properties of the white dwarf population is the white dwarf luminosity function, which is defined as the number of white dwarfs per cubic parsec as a function of unit luminosity. The white

4

dwarf luminosity function not only can provide valuable information about the age, structure and evolution of our Galaxy but it also provides an independent test of the theory of dense plasmas (Isern et al., 1997, 1998a). Also, it directly constrains the current death rate of low- and intermediate-mass stars in the local neighborhood which, in turn, provides an important constraint on pre-white dwarf stellar evolutionary sequences. However, in order to use the white dwarf luminosity function to study these interesting astrophysical problems, it is necessary to have good observational data, accurate stellar models, and reliable prescriptions to model the population components of our Galaxy. In this paper we review the current knowledge of the white dwarf luminosity function, from both the observational and theoretical points of view.

The paper is organized as follows. Section 2 reviews the observational efforts, while in Sect. 3 we provide an overview of the theoretical models. It is followed by Sect. 4, where we discuss the current state of the art of the white dwarf cooling theory, paying special attention to the most relevant evolutionary phases. For the sake of brevity, we will not review in detail the abundant theoretical background, but only those salient features of the theory needed to model the white dwarf luminosity function. The interested reader is referred to Renedo et al. (2010) and Althaus et al. (2010a) for detailed discussions on topics such as the so-called convective coupling or spectral evolution. In Sect. 5 we discuss other important inputs necessary to model the white dwarf luminosity function. In Sect. 6 we elaborate on a few of the many astrophysical applications of the white dwarf luminosity function. Section 7 outlines the foreseeable future research in the field from both the theoretical and observational points of view. Finally, Sect. 8 summarizes in a comprehensive way the most relevant observational results previously analyzed in Sect. 2, and lists the ages of the Galactic disk derived from the observed luminosity functions. We conclude with a general summary, which is presented in Sect. 9.

Before going into details we would like to stress that the selection of papers for explicit citation may be somewhat incomplete, as the field is rapidly evolving, and moreover it is the product of the special research trajectory of the authors. We apologize in advance for any unintentionally missed references.

2. The observed white dwarf luminosity function

Over fifty years ago it was first recognized that the coolest (faintest) white dwarfs are remnants of the earliest stars to form in the Solar neighborhood (Schmidt, 1959), and that cooling theory could be used to estimate the time elapsed since star formation commenced in the Galactic disk (Mestel, 1952; van Horn, 1968). Three decades later, the white dwarf luminosity function helped resolve serious discrepancies between the ages of the oldest stars in the Galaxy and the age of the Universe implied by the Hubble recession rate of galaxies (Watson, 1998; Lineweaver, 1999). Following on the heels of these pioneering works, several other investigations began to use white dwarfs as reliable cosmochronometers to determine ages of individual stars, binaries and stellar clusters — see Fontaine et al. (2001) for an excellent review of this topic.

The observed white dwarf luminosity function preserves a record of the star formation and death rate that spans the history of the Galaxy, sets constraints on the quantity of its local baryonic matter, the recycling of material to the interstellar medium, and encodes the kinematics of stellar populations throughout the disk and halo. Its uses and inherent limitations have been discussed in a number of excellent papers (Weidemann, 2000a; Méndez and Ruiz, 2001; Bergeron et al., 2001; Hansen and Liebert, 2003), while several reviews of the theory behind the white dwarf luminosity function provided essential caveats and context for its interpretation (D'Antona and Mazzitelli, 1989; Koester, 2002).

Those new to the topic of the white dwarf luminosity function would do well to start with the above references as background. Here we focus on a few key developments leading to the present state of the empirical white dwarf luminosity function and what can be expected in the near future. A comprehensive summary of all relevant work is well beyond the scope of this review. We apologize in advance if a particular project of interest has been omitted. However, each of the works cited below contains an abundance of references and comparisons, details on the methods employed and, especially, the myriad pitfalls associated with constructing an empirical luminosity function for white dwarfs.

Any observational study of the white dwarf luminosity function must begin with a well-defined sample. In the work summarized below, three basic approaches have been used. One is to identify a magnitude-limited sample using color index selection criteria to isolate the most likely white dwarf

candidates. Another approach is to use proper motions and color indices to isolate nearby white dwarf candidates by their intrinsic low luminosity, color and high proper motion. Such samples usually require a weighting scheme to correct for the kinematic bias that causes fast-moving distant and slow-moving nearby objects to be undercounted. The best approach is to do straightforward counts in a large volume-limited sample that is demonstrably complete. Unfortunately, this is rarely possible due to the low luminosity of white dwarfs, confusion of the cooler ones with lower main sequence stars and sub-dwarfs, the lack of spectra for many objects, and the lack of precision trigonometric parallaxes.

In the works described below all three of these approaches have been used. The discussion is arbitrarily organized into five parts and presented in rough chronological order within each part. Section 2.1 outlines several key attempts to quantify the more accessible hot (bright) end of the white dwarf luminosity function, which constrains the current white dwarf formation rate. Section 2.2 provides an overview of early (pre-2000) efforts to construct the full white dwarf luminosity function from local samples of white dwarfs. Section 2.3 describes more recent progress towards a definitive luminosity function for the local white dwarf sample. This work has tended to take two approaches: construction of complete nearby samples of white dwarfs that are effectively limited to the thin disk and searches within large modern surveys that include white dwarfs from a mix of populations (thin disk, thick disk, halo). Section 2.4 describes very preliminary attempts to construct the luminosity function specifically for the halo (spheroidal) population of white dwarfs. Section 2.5 provides some concluding remarks on key issues that still need to be addressed, as well as prospects for improving the observed white dwarf luminosity function in the near future.

2.1. The hot end of the white dwarf luminosity function

The hot DA white dwarfs in the Palomar-Green (PG) Survey (Fleming et al., 1986) comprise a magnitude-limited sample originally selected primarily on the basis of blue color criteria. This sample was used to anchor the hot end of one of the first estimates of the full white dwarf luminosity function (Winget et al., 1987; Liebert et al., 1988) discussed below. The PG sample of hot white dwarfs, i.e., those brighter than $M_v = 13$, was analyzed by Liebert et al. (2005) using high signal-to-noise spectra and improved atmosphere model fits to the Balmer lines to derive temperatures, gravities,

masses, radii and cooling ages. Their luminosity function, corrected for incompleteness and weighted by the $1/\mathcal{V}_{\mathrm{max}}$ method (Schmidt, 1968) indicated that hot white dwarfs comprise about ten percent of the white dwarf space density. This careful study is most noteworthy for its examination of apparent structure in the white dwarf mass distribution and for one of the first robust determinations of the formation rate of white dwarfs with hydrogen-rich atmospheres. The latter constrains the formation rate and space density of planetary nebulae and, consequently, stellar evolutionary models for progenitors less than about ten solar masses.

The Kiso Schmidt survey of UV-excess objects (Kondo et al., 1984) also proved to be a rich source of hot white dwarfs. Using this magnitude- and color-limited sample, supplemented by their own spectroscopic identifications, Wegner and Darling (1994) published one of the first white dwarf luminosity functions based on this survey. Their luminosity function and space density of hot white dwarfs were found to agree well with that derived from the PG sample.

In a preliminary analysis of the Anglo-Australian Telescope 2dF QSO Redshift Survey (2QZ) data, Vennes et al. (2005) identified $\sim 2,400$ white dwarf candidates at distances up to 1 kpc above the Galactic plane. The main thrust of this work was to measure both the scale height and luminosity function for hot white dwarfs. A white dwarf luminosity function was presented for stars brighter than $M_v \sim 13$. It matches the early white dwarf luminosity function of Fleming et al. (1986) and has a similar scale height (200-300 pc). Notably, the 2QF sample appears to be complete at the bright end, i.e., for $10 < M_v < 12.5$.

The hot end of the white dwarf luminosity function was evaluated using the Sloan Digital Sky Survey (SDSS) DR4 data by Krzesinski et al. (2009). This well-calibrated large sample included almost 6,000 stars. It enabled a thorough examination of incompleteness and other systematic effects, though they did not attempt to derive a disk age or space density. They also identified a plateau between $0.5 \leq M_{\mathrm{bol}} \leq 3.8$. Torres et al. (2014) found that this plateau could not be the result of a sudden change in the white dwarf birth rate because it would also be visible in the luminosity function of helium-rich white dwarfs. Once stars with masses smaller than the canonical limit for the formation of a carbon-oxygen white dwarf were removed from the observational sample the agreement between theory and observation was nearly perfect (Torres et al., 2014; Krzesinski et al., 2015).

The DA/non-DA ratio as a function of luminosity is an important con-

straint on the evolutionary channels that govern the atmosphere transformations and chemical composition changes as the hottest white dwarfs cool. However, hot white dwarfs are quite rare and this leads to large errors in the observed DA/non-DA ratio at the hot end of the luminosity function. Spectral features tend to be weak or absent in cooler white dwarfs, making this ratio difficult to determine, underscoring the importance of the hot white dwarf luminosity function as a fundamental constraint on the spectroscopic evolution of cooling white dwarfs that influences the entire luminosity function. However, temperatures for some of the hot DA white dwarfs can be overestimated due to unknown atmospheric metal abundances; shifting them to lower luminosity bins changes the shape of the hot white dwarf luminosity function and the DA/non-DA ratio.

Limoges and Bergeron (2010) presented an analysis of the hot DA and DB white dwarfs in the Kiso Schmidt survey, using detailed model atmosphere fits to the optical spectroscopic data. The resulting M_v values were compared with the original estimates of Darling (1994), which were obtained from empirical photometric calibrations. Limoges and Bergeron (2010) found the two approaches (spectra and photometry) had a relatively small impact on the calculated luminosity functions. They also determined separate luminosity functions for DA and DB stars and placed a smaller number of stars in the fainter magnitude bins than Darling (1994). The luminosity functions, space densities and completeness determinations they obtained from the Kiso sample were found to be quite consistent with those published by Liebert et al. (2005) for the PG survey, establishing the hot end of the observed white dwarf luminosity function as a reliable constraint on deeper investigations. Of particular note, however, Limoges and Bergeron (2010) discovered several unresolved double-degenerate binaries in the sample, raising the possibility that other undetected pairs have affected estimates of the space density of white dwarf stars in studies that do not use detailed atmospheric model fits to spectra.

Krzesinski (2013) noted that removing low mass white dwarfs from their sample increases the DA/non-DA ratio at high effective temperatures as well as in the range known formerly as the DB gap. He suggested that a new SDSS white dwarf catalog from a later data release could provide a large enough basis to begin to address these problems.

In summary, because it fully incorporates new theoretical models for white dwarf atmospheres, cooling, completeness, biases and selection effects, the work outlined above — see additional references in Krzesinski et al. (2015)

— can be regarded as the most definitive determination of the hot white dwarf luminosity function at the moment. The PG and Kiso surveys continue to be valuable touchstones for evaluating selection effects and completeness of newer samples of hot white dwarfs. Indeed, these white dwarfs are often embedded in the larger newer studies. Current samples are now so large that it is no longer observationally necessary to consider the hot end of the white dwarf luminosity function as a separate project. The following sections outline attempts to fully determine the white dwarf luminosity function to and beyond an expected downturn in space density at $M_{\mathrm{bol}} \sim 15$.

2.2. Early work on the full white dwarf luminosity function for the Galactic disk

To the best of our knowledge, the first attempt to construct an observational white dwarf luminosity function was made in the late sixties (Weidemann, 1967). Using three datasets (Luyten, 1958, 1963; Eggen and Greenstein, 1965), Weidemann (1967) demonstrated that all closely followed the expected cooling theory (Mestel and Ruderman, 1967). Assuming an age of 10 Gyr for the Galaxy, it was estimated that white dwarfs as faint as $M_{\mathrm{bol}} \sim 16.5$ should have been found. At that time, none fainter than $M_{\mathrm{bol}} \sim 15$ were known. In hindsight, it was the low quantum efficiency of photographic plates and early electronic detectors that frustrated early searches for faint (cool) white dwarfs — see Liebert et al. (1979) and Greenstein (1986a,b).

Many of the early white dwarf luminosity functions were constructed from Luyten's landmark proper motion surveys (Luyten, 1963). Luyten used second-epoch red plates taken about a decade after the original Palomar Observatory Sky Survey (POSS-I) to measure proper motions, photographic magnitudes, and crude color classes for stars down to the plate limit near $m_{\mathrm{pg}} \simeq 21$ for roughly two-thirds of the sky. With these data he identified candidate white dwarfs using so-called reduced proper motion diagrams, a technique for isolating stellar populations he pioneered (Luyten, 1922) — see Jones (1972) for an early assessment of this technique. Later, with new high quantum efficiency instrumentation this sample proved to contain many of the previously "missing" cool faint white dwarfs (Hintzen, 1986; Oswalt et al., 1988).

Over thirty years ago, it was pointed out by Liebert (1979) that the observed scarcity of white dwarfs of very low luminosity could be due to either large errors in the cooling theory, or to the finite age of the Galaxy. This idea was first tested by Winget et al. (1987). Using a sample of 43

spectroscopically identified white dwarfs with trigonometric parallax data they concluded that the absence of stars in the lowest luminosity bin was statistically significant. Expanding on this idea, the Luyten Half-Second Catalog (Luyten, 1975; Liebert, 1979) — a subset of Luyten's POSS-I proper motion survey – was used for a more detailed analysis of the white dwarf luminosity function by Liebert et al. (1988). A sample of mostly cool white dwarfs with $\mu > 0.8$ sec yr^{-1} and $M_v > 13$ was selected to better distinguish nearby low luminosity white dwarfs from high velocity background stars. To maximize completeness, hot white dwarfs were added from the color-selected PG sample of Fleming et al. (1986). There was initial concern that the Liebert et al. (1988) sample was not complete, especially at the critical faint end that constrains the age of the Galaxy (Iben and Laughlin, 1989; Oswalt et al., 1996; Flynn et al., 2001). In a more complete sample, the position of the downturn would move to fainter magnitudes and hence the Galactic age determination would increase. However, many of the fields were re-examined by Monet et al. (2000) using new POSS-II plates and it was concluded that the LHS sample is roughly 90 percent complete over the magnitude and proper motion limits used in Liebert et al. (1988), when the scale height of the Galaxy is taken into account. This sample provided the first reliable estimate for the local mass density of white dwarfs and a minimum age for the Galactic disk of ~ 9 Gyr.

The Luyten POSS-I survey was also used by Oswalt et al. (1996), but with a different approach. A large sample of wide binaries containing spectroscopically identified white dwarfs with much fainter magnitudes and much smaller proper motions were selected. This permitted the sample to be as deep as possible and also to include any nearby slow moving white dwarfs that would have been overlooked by Liebert et al. (1988). Corrections for incompleteness in the sample were made by constructing star counts vs. both magnitude bin and proper motion bin. $BVRI$ photometry was used to estimate the white dwarf luminosities by interpolating within the grids of hydrogen-rich and helium-rich atmosphere cooling models by Wood (1995). The model chosen to determine the luminosity for each of the ~ 50 stars in the sample was determined by the dominant constituent seen in its spectrum. A mass of $0.6\,M_\odot$ was assumed for stars without independent mass determinations. The uncertainty in composition and the empirical dispersion in the white dwarf mass distribution published by Bergeron et al. (1992) were included in the error analysis. This study revealed that the downturn was less steep than found by Liebert et al. (1988), implying a somewhat older

minimum age of ~ 9.5 Gyr for the Galactic disk.

Leggett et al. (1998) obtained optical and infrared data for the sample of Liebert et al. (1988). Using model atmospheres by Bergeron et al. (1995) and new trigonometric parallaxes, they recomputed the white dwarf luminosity function. The result yielded only slight differences in the shape and a modest increase in disk age from Liebert et al. (1988). Incorporation of improved trigonometric parallaxes (the dominant uncertainty in luminosity estimates) and additional leverage on atmospheric composition provided by the infrared data for the cooler objects, made the Leggett et al. (1998) a more definitive determination of the white dwarf luminosity function than prior work.

Knox et al. (1999) constructed one of the first white dwarf luminosity functions not based on the Luyten proper motion survey. Digital scans of ~ 300 SuperCOSMOS ESO/SERC plates were used to identify white dwarf candidates via reduced proper motion diagrams. Both the proper motion and photographic color estimates were much improved over what Luyten could do with the POSS plates. More importantly, a special effort was made to assess the incompleteness of the sample of 58 white dwarf candidates that were identified. It is one of very few samples shown to pass the $\langle 1/\mathcal{V}_{\mathrm{max}}\rangle = 0.5$ completeness test (Schmidt, 1975a). The atmosphere models of Bergeron et al. (1995) were used to estimate the white dwarf candidates' luminosities. The magnitude and proper motion limits of this survey significantly exceeded that of Leggett et al. (1998), enabling the detection of intrinsically fainter stars. The downturn at the faint end of the white dwarf luminosity function was found to be more gradual than most earlier surveys, implying a minimum disk age of ~ 9.5 Gyr, in accord with the findings of Oswalt et al. (1996).

The white dwarf luminosity function was re-evaluated by Smith (1997) and summarized by Smith et al. (2003) using much-improved photometric and spectroscopic data for a sample of Luyten white dwarfs in wide binaries more than three times larger than used in Oswalt et al. (1996). Using the same incompleteness correction strategy and the $1/\mathcal{V}_{\mathrm{max}}$ methodology, the revised luminosity function, space density and disk age were unchanged. However, the larger sample improved the precision of each by about a factor of two.

The above studies marked important stepping stones towards a definitive white dwarf luminosity function. Because of its tie to good trigonometric parallaxes and careful fitting of atmospheric models to the white dwarf spectral energy distributions, the luminostiy function of Leggett et al. (1998) probably is the best early benchmark. However, the work by Oswalt et al. (1996)

and Knox et al. (1999) convincingly demonstrated that deeper surveys were needed to delineate the faint end of the white dwarf luminosity function that constrains the age of the Galaxy and to identifying the fraction of each bin contributed by its halo components. These issues spurred the more recent work using large modern surveys, which are addressed in the next two sections.

2.3. The disk white dwarf luminosity function: balancing quality and quantity

Newer work on the white dwarf luminosity function has tended to focus on obtaining "quality", i.e. well-vetted complete samples of nearby white dwarfs drawn from a variety of sources, or "quantity", i.e. large samples of white dwarfs gleaned from huge surveys with well-quantified completeness characteristics. We begin this section with some examples of the first type.

Only within the last decade or so has the census of nearby white dwarfs grown large enough to seriously pursue the best way to determine a luminosity function: direct star counts by volume. Holberg et al. (2008) used the Catalog of Spectroscopically Identified White Dwarfs (McCook and Sion, 1999) to identify a sample of well over 100 white dwarfs with high quality spectra, photometry, proper motions and parallaxes likely to be within 20 pc of the Sun. Their subset of 44 white dwarfs within 13 pc of the Sun was shown to be essentially complete and the 20 pc sample as a whole was shown to be almost 80 percent complete. Thus, simple star counts could be used to derive the space density. This avoids the necessity of using the $1/\mathcal{V}_{\max}$ method or more sophisticated statistical methods, all of which are susceptible to small number fluctuations, observational biases, and/or unproven completeness — see Wood and Oswalt (1998) for a discussion of these problems.

The kinematical properties, spectroscopic subtypes and stellar population subcomponents of the 20 pc local white dwarf sample were evaluated by Sion et al. (2009). Virtually the entire sample was found to belong to the thin disk component of the Galaxy. This local sample contained not a single interloping member of the halo. Sion et al. (2014) confirmed these results in an expanded sample of over 200 white dwarfs within 25 pc. The completenesss of these samples were shown to be well-behaved functions of distance, from nearly 100% at 13 pc, to 85% at 20 pc, to 60% at 25 pc. They provide useful benchmarks against which to assess and compare samples comprised of more distant white dwarfs.

Other groups have been working hard to extend and complete the local white dwarf sample. Giammichele et al. (2012) performed a detailed photo-

metric and/or spectroscopic analysis of every white dwarf suspected to lie within 20 pc of the Sun. The sample was mostly drawn from the 20 pc list given in Sion et al. (2009). The sample completeness was estimated to be about 90%. While it agrees well with the work cited above in the low luminosity bins, at higher luminosities (white dwarfs hotter than about $T_{\mathrm{eff}} = 12,000$ K) an apparent over-density of a factor of two relative to these other luminosity functions was of concern. Most likely, this was due to the small number of stars (< 10) in the brighter bins, a hypothesis that can only be tested with much larger samples.

Holberg et al. (2016) completed a new analysis of the 25 pc sample, expanding the count of spectroscopically identified white dwarfs by about a factor of two relative to the original 20 pc sample. This expanded sample provided evidence that single white dwarfs are significantly more represented than those with one or more companions, suggesting that some companions are lost to mergers or escape during post-main sequence evolution. In addition, this study provided the first estimate of the white dwarf birthrate as a function of time from ~ 8 Gyr ago to the present, indicating that the present production of white dwarfs is a factor of two to three higher than the average over this period. If mergers contributed a significant component to the white dwarf population or the birthrate has changed significantly in the Galaxy these effects will need to be considered in interpreting the white dwarf luminosity function. These concerns notwithstanding, the Holberg et al. (2016) white dwarf luminosity function obtained by simple number counts is in good agreement with prior work and should be considered a more fundamental determination.

In parallel with studies focused on the luminosity function of the nearby sample of white dwarfs, much effort has been put into quantifying it using huge samples of white dwarf candidates drawn from large new surveys. We now summarize a few of the most significant "quantity-based projects".

The Luyten sample still has potential to improve the white dwarf luminosity function. Salim and Gould (2002, 2003) used the NLTT positions, magnitudes and colors to cross-correlate to the 2MASS and USNO-A survey data to construct a catalog of white dwarf candidates in the overlap of regions covered by these surveys. The improvements in proper motion estimates and photometric indices derived from the 2MASS J-band and estimated photographic V magnitudes from the NLTT permitted construction of reduced proper-motion diagrams that cleanly separate the main sequence, subdwarfs, and white dwarfs. The task of obtaining high quality spectroscopic identifi-
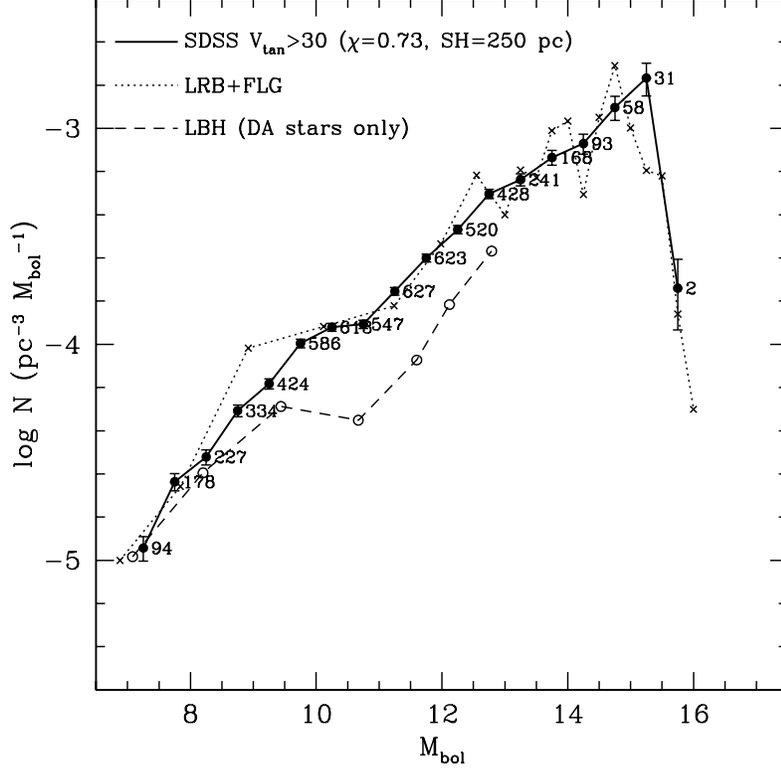
Figure 1: Luminosity function of disk white dwarfs derived from the Sloan Digital Sky Survey (SDSS), from Harris et al. (2006), compared to the luminosity functions of Leggett et al. (1998) and Liebert et al. (2005).

cations and cross-correlated *ugriz* photometry for nearby cool white dwarfs in the NLTT catalog was undertaken by Kawka and Vennes (2006) but, to date, it does not appear that a white dwarf luminosity function has been constructed for this spectroscopically identified portion of the sample.

Harris et al. (2006) constructed a white dwarf luminosity function using proper motions based on comparison of positions between the SDSS and USNO surveys, high quality *ugriz* photometry, and improved atmospheric models. As shown in Fig. 1, the resulting white dwarf luminosity function is surprisingly smooth and drops off abruptly at $M_{\rm bol} = 15.3$. Because of the scarcity of stars in bins beyond the downturn, no attempt was made to derive the age of the disk or the space density of white dwarfs. Both Harris et al.

(2006) and Kilic et al. (2006) attempted to address the incompleteness of the SDSS white dwarf sample as well as the effects of contamination by other types of stars and unresolved components, but in fact the SDSS does not adequately sample the nearby population of white dwarfs due to the original surveys bright limit, nor does it go deep enough to delineate the downturn. Incidentally, the Vennes et al. (2005) hot white dwarf candidates mentioned above have been shown to be from the same parent population sampled in the northern hemisphere by Harris et al. (2006). Thus, it provides an important supplement to the incompleteness of the SDSS at the bright end of the luminosity function.

Limoges et al. (2013) examined the white dwarf population within 40 pc of the Sun using a spectroscopic survey of northern hemisphere candidates from the SUPERBLINK proper motion database. The expanded survey subsequently evaluated by Limoges et al. (2015) is between 66 and 78% complete. It contains almost 500 white dwarfs, an order of magnitude more than the original Liebert et al. (1988) luminosity function. Using a set of homogeneous model atmospheres, they found an unexpectedly large fraction of massive white dwarfs. These less luminous objects at the faint end of the luminosity function were often missed by previous surveys. Like Giammichele et al. (2012) the disk white dwarf luminosity function obtained from this sample also has an apparent excess of hot white dwarfs, most likely due to contamination by non-DA white dwarfs as in the Krzesinski (2013) sample. The Limoges et al. (2015) luminosity function is the only one based on a 40 pc volume-limited sample. However, trigonometric parallaxes are still needed to clearly define the shape of the faint end of the luminosity function where the disk and halo white dwarfs mingle.

Torres and García-Berro (2016) simulated the Limoges et al. (2015) survey. They were able to reproduce the observed white dwarf luminosity function quite well and showed the sample completeness is typically $\sim 80\%$, for $M_{\mathrm{bol}} < 16$, beyond which it drops rapidly below 20%. They also demonstrated that the downturn in the observed luminosity function located at $M_{\mathrm{bol}} \sim 15$ is statistically robust. Using new progenitor evolutionary models and cooling sequences to model the white dwarf luminosity function constructed from the Limoges et al. (2015) sample, they determined the age of the Solar neighborhood to be about 8.9 ± 0.2 Gyr, about a factor of two more precise than the best prior age determinations. This estimate was shown not to depend significantly on the slope of the initial mass function or the adopted initial-to-final mass relationship. However, the peak in the

luminosity function was found to be shaped by a steeper initial-to-final mass relation for progenitor masses larger than about $4\,M_\odot$. An apparent bump in the luminosity function near $M_{\rm bol} \sim 10$ was found to be significant and most likely the result of a recent burst of star formation about 0.6 ± 0.2 Gyr ago that continues to the present era. This is roughly in accord with the empirical results of Holberg et al. (2016) derived from the 25 pc sample.

Another significant step towards a definitive observed white dwarf luminosity function is the study of DA white dwarfs identified in the LAMOST (Large Sky Area Multi-Object Fiber Spectroscopic Telescope) Spectroscopic Survey of the Galactic anticenter (LSS-GAC) by Rebassa-Mansergas et al. (2015). Their study followed a well-defined set of criteria for selecting targets for observations, in contrast to other large surveys with target selection algorithms complicated by other scientific goals that make it difficult to quantify the observational biases influencing the observed populations of white dwarfs. Even so, Gentile Fusillo et al. (2015) determined that the Rebassa-Mansergas et al. (2015) survey's incompleteness is too large in the faintest bins to confidently extend the luminosity function beyond the downturn.

To summarize this section, the luminosity function of disk white dwarfs has been the subject of a number of studies employing different approaches. Over the luminosity bins in common, all of them agree within the uncertainties quoted by each of the surveys. All have consistently found that, beginning with its bright (hot) end, the white dwarf luminosity function increases monotonically with increasing bolometric magnitudes at a nearly constant slope (which stems from the cooling law), and terminates with an abrupt downturn near $M_{\rm bol} \sim 15$ (a consequence of the finite age of the Galactic disk). Enticing but very preliminary evidence for fine structure in the white dwarf luminosity function suggests that the star formation rate in the solar neighborhood has not been constant. At present, because of its large sample size and all the work that has been put into quantifying its systematic errors, incompleteness and biases, the SDSS-based Harris et al. (2006) white dwarf luminosity function is the best benchmark against which newer studies should be compared.

2.4. In search of the halo white dwarf luminosity function

It was early noted (Schmidt, 1959) that the white dwarf luminosity function could give useful constraints on the age and mass density of the Galactic halo. The importance of detecting and characterizing this population of the

Galaxy's oldest stars to such questions as the age of the halo and to the nature of detected MACHO events has been reviewed by Fontaine et al. (2005). In one of the first attempts, Liebert et al. (1989a) used just six stars with high space motions to construct a preliminary halo white dwarf luminosity function. Since then, only modest increases have been achieved in the number of confirmed halo white dwarfs, because they comprise such a rare component of the solar neighborhood. In addition, the detection of halo white dwarfs is hampered by the difficulty of obtaining their three dimensional kinematical properties. Sophisticated neural network techniques may prove to be useful in addressing these problems (Torres et al., 1998). However, radial velocities are difficult to measure for single white dwarfs because of their sizable gravitational redshifts and frequent lack of measurable absorption lines, making full three-dimensional kinematics hard to come by. This, in turn, results in difficulty distinguishing between thick disk and halo white dwarfs (Pauli et al., 2003, 2006).

The theoretical prediction (Hansen, 1999; Saumon and Jacobson, 1999) and observational confirmation (Harris et al., 1999; Farihi, 2004) of depressions in the near-IR spectra of very cool white dwarfs underscored the need for improvements in cool atmosphere models as well as better observational data. Below about 4,500 K, the infrared colors of white dwarfs with hydrogen-rich atmospheres become bluer as cooling progresses, due to broad opacity sources such as collisionally induced absorption by hydrogen molecules. This immediately caused concern that the fainter bins in some of the white dwarf luminosity function determinations might contain stars whose luminosities had been based on erroneous photometric parallaxes or atmospheric models.

The discovery of "cool blue degenerates" sparked renewed interest in finding old halo white dwarfs in the solar neighborhood. For example, the large space densities reported by Ibata et al. (1999) and Oppenheimer et al. (2001) ignited a flurry of excitement at the prospect that ancient white dwarfs might comprise most or all of the Galaxys dark matter content. Most of these objects were subsequently shown to be the result of misidentifications of thick disk white dwarfs and/or stars of indeterminate proper motion — see Reid et al. (2001), Silvestri et al. (2002), and references therein. Ultimately, no real improvement in the halo white dwarf luminosity function was obtained.

In an attempt to find halo white dwarfs, Majewski and Siegel (2002) applied the reduced proper motion technique to a "pencil beam" sample of over 800 faint stars ($B < 22.5$) with proper motions of high precision in a 0.3

square degree field near the north Galactic pole. Eight white dwarf candidates were identified in this field. Taking into account the narrowness of the field and the much smaller areal density of nearby white dwarfs across the sky, they concluded that a substantial faint population of white dwarfs may extend well above the scale height of the Galaxy without significantly affecting the local white dwarf space density. Their maximum likelihood method was shown to be far less sensitive to small number fluctuations that affect the $1/\mathcal{V}_{max}$ method used by nearly all other investigations of the white dwarf luminosity function.

A robust white dwarf luminosity function for the halo should contain at least as many stars (~ 50) as the early white dwarf luminosity functions for the disk. This immediately brings to mind large surveys such as the SDSS. However, despite a much larger sample size, the original SDSS does not probe as deeply as the original Liebert et al. (1988) study. Among spectroscopically identified white dwarfs in the SDSS, Hu et al. (2007) showed that the sample is complete only between $16 < g < 18$. This is not surprising, since stars were not the primary targets of the SDSS. This sample is therefore subject to very complex selection effects that are strong functions of magnitude, area, color, position in the sky and other factors — see Gentile Fusillo et al. (2015). Despite these obstacles, Hu et al. (2007) were able to derive improved estimates for the DA white dwarf space density and formation rate that are in good agreement with prior values.

The SuperCOSMOS and RECONS surveys (Hambly et al., 2004; Subasavage et al., 2005) were aimed at detecting halo white dwarfs. They identified ~ 104 new candidate white dwarf stars, almost two orders of magnitude larger than the first samples used to determine the white dwarf luminosity function several decades ago. Rowell and Hambly (2011) used this sample to estimate the space density of white dwarfs in the halo. Although the majority lack spectroscopic confirmation, the colorimetric and reduced proper motion criteria used to identify candidates were shown to be reliable; known white dwarfs in the sample were readily identified. Importantly, this group introduced a new technique to convincingly distinguish the disk and halo white dwarfs for the first time, extending the search to 1.0 and 2.5 magnitudes deeper, respectively, than the SDSS study of Harris et al. (2006). Their results confirm the location of the downturn in the disk white dwarf luminosity function near $M_{bol} = 15.75$. They also concluded that the different kinematic populations overlap so seriously beyond the peak in the disk white dwarf luminosity function that traditional approaches to constructing one cannot render a more

accurate (thin) disk age at the present time and only a very preliminary halo age of 11–12 Gyr.

In view of the large sample size and care taken to account for incompleteness, quantify selection effects and unravel population mixing, the Rowell and Hambly (2011) white dwarf luminosity functions for the thin disk, thick disk and halo are the best currently available for these population components.

2.5. Prospects for improving the disk and halo white dwarf luminosity functions

The various studies outlined above have determined the white dwarf luminosity function for thin disk members to a precision of a few percent for stars brighter than the downturn near $M_{bol} \sim 15$. Most of the ongoing and planned surveys seek to find enough white dwarfs to populate the lowest luminosity bins of the luminosity function where the disk and halo populations are currently hopelessly mixed, and mired in small number statistical uncertainties. Many of these white dwarfs are likely be the "cool blue degenerate stars" noted above, if they have hydrogen-rich atmospheres. Whether they are the dominant component of the halo white dwarf population remains to be seen. This has been a topic of considerable debate — see Camacho et al. (2007), Torres et al. (2008) and Torres et al. (2010).

Gentile Fusillo et al. (2015) pointed the way to better use of the SDSS for constructing the white dwarf luminosity function. Using the SDSS DR10, they developed a selection method for white dwarfs that reliably identified white dwarf candidates based on SDSS colors and reduced proper motion. From a large sample of spectroscopically confirmed white dwarfs and known contaminants (i.e., non-white dwarfs) drawn from the SDSS DR7 they devised a method of computing the probability of being a white dwarf for any object having only multiband photometry and proper motion data. The spectroscopic sample was limited to bright objects ($g < 19$) for which reliable proper motions could be obtained from prior photographic plates. Applying the technique to the SDSS DR10 photometric catalogue, they selected $\sim 23,000$ high-confidence white dwarf candidates, of which $\sim 14,000$ lacked spectra. On average, the sample was found to be only about 40 per cent complete for white dwarfs hotter than $T_{eff} \simeq 7,000$ K and brighter than $g \simeq 19$. While they did not attempt to construct a white dwarf luminosity function, their results underscored both the remaining potential of the SDSS for improving it, as well as the continuing need for follow-up spectroscopy.

Almost 40,000 white dwarfs now have been spectroscopically identified in the various extensions of the SDSS, up through its 12th Data Release (Alam et al., 2015). Among these are several thousand new white dwarfs identified by Kepler et al. (2015) in the SDSS DR10. Using the best SDSS spectra and the latest atmospheric models they computed temperatures, gravities, and atmospheric abundances for several thousand hydrogen atmosphere white dwarf stars (DAs), several hundred helium atmosphere white dwarf stars (DBs), as well as dozens of white dwarfs with metallic lines (DZs) and white dwarfs with carbon dominated spectra (DQs). They also constructed the best currently available white dwarf mass distribution using model fits to high quality SDSS spectra for $\sim 6,000$ DAs and corrected for the observed volume via the $1/\mathcal{V}_{\mathrm{max}}$ method.

The Kepler et al. (2015) identifications reach to $T_{\mathrm{eff}} = 5,000$ K, although in this regime the sample is certainly not complete, as they relied on proper motion measurements (known to be incomplete below $g \sim 21$) to distinguish between cool DCs and BL Lac objects. However, this huge increase in the number of spectroscopically confirmed white dwarfs is important because it enabled discovery of many rare objects such as massive white dwarfs, magnetic white dwarfs, and He-dominated objects with oxygen lines, unresolved binaries,...Of special note, they compiled a list of nearly 100 white dwarf stars with masses above $1\,M_\odot$ and found that the volume corrected distribution is inhomogeneous. If confirmed, this may imply mergers are a significant contributor to the white dwarf luminosity function.

While neither presented new determinations of the white dwarf luminosity function, the Gentile Fusillo et al. (2015) and Kepler et al. (2015) studies are important steps to this goal and their strategies could be applied to even larger future samples. Compared to previous work they followed much more well-defined criteria for selecting targets. Their assessments also revealed that the incompleteness at the bolometric magnitudes typical of the downturn in the luminosity function is still large, and thus more work with still larger samples will be required to derive a reliable luminosity function at faint magnitudes. Sayres et al. (2012) demonstrated that a multi-survey approach can improve detection of nearby faint white dwarfs of low proper motions and rejecting contaminating populations of stars.

In summary, substantial improvement in the present state of the observed white dwarf luminosity function will require several advancements in both the quality and quantity of the observational data, as well as improvements in the models used to construct and interpret it:

1. An ultra large sample of white dwarfs, on the order of 10^5 stars.
2. Precise parallaxes, substantially better than 1 mas.
3. Precise proper motions, substantially better than 1 mas/yr.
4. High quality photometry for a magnitude-limited sample to at least $g \sim 21$.
5. Spectroscopic identifications of sufficient resolution for velocity determinations.
6. Improved atmospheric models for very cool white dwarfs.
7. Improved spectral evolutionary models.
8. Better categorization and treatment of selection effects.
9. Quantification of the effects of unresolved binaries and high mass white dwarfs.

Some of the above requirements can be met by existing surveys such as the expanded SDSS. Until Gaia, however, it is unlikely that a truly definitive white dwarf luminosity function for either the disk population components or halo will be achieved, primarily since precision parallaxes and proper motions are essential to proper bin assignment and resolution of the various populations that mix at the faint end of the observed white dwarf luminosity function. This is an intractable problem for the current surveys. In short, the downturn in the disk luminosity function for now is ill determined below about $10^{-4} L_\odot$. Further, because they comprise a tiny fraction of the local population, a complete (or at least a very well-behaved incomplete) sample of white dwarfs needs to be constructed to distances approaching 1 kpc in order to capture a statistically significant number of faint halo white dwarfs. Torres et al. (2005) estimate that Gaia will find 250,000 to 500,000 white dwarfs — see also Carrasco et al. (2014). This will open a whole new era of research on the white dwarf luminosity function.

3. Theoretical models of the white dwarf luminosity function

The white dwarf luminosity function can be formulated as

$$n(L) \propto \int_{M_\mathrm{i}}^{M_\mathrm{s}} \Phi(M) \, \Psi(T - t_\mathrm{cool}(L, M)$$
$$-t_\mathrm{MS}(M)) \tau_\mathrm{cool}(L, M) \, dM \tag{3}$$

where L is the luminosity, M is the mass of the parent star (for convenience all white dwarfs are usually labelled with the mass of their main sequence progenitor), t_{cool} is the cooling time necessary to reach a luminosity L, $\tau_{\mathrm{cool}} = dt_{\mathrm{cool}}/dM_{\mathrm{bol}}$ is the characteristic cooling time, t_{MS} is the main sequence lifetime of the progenitor of the white dwarf, and T is the age of the population under study. The remaining quantities, the initial mass function, $\Phi(M)$, and the star formation rate, $\Psi(t)$, are not known *a priori* and depend on the physical properties of the stellar population under study. For context, excellent fundamental reviews of how the luminosity function can be constructed for more general spectral types and population groups can be found in Mihalas and Binney (1981) and Binney and Merrifield (1998).

Obviously, both the cooling time and the characteristic cooling time must be obtained from detailed cooling sequences. Clearly, the cooling rates are crucial in determining the white dwarf luminosity function. When the characteristic cooling time increases (small cooling rates) the number of white dwarfs per unit volume correspondingly increases. This occurs when either there is an additional release of energy in the core — such as the release of latent heat upon crystallization, see below — or when an additional source of opacity in the atmosphere appears. The reverse is also true. For instance, when neutrinos are copiously produced in the deep interior of the white dwarf the cooling rates are large, hence the white dwarf luminosity function drops below the nominal value when only the contribution due to heat capacity is taken into account.

The main-sequence lifetime and a relation between the mass of the progenitor stars and the mass of the white dwarf itself must also be provided (this is known as the initial-final mass relationship). Usually, these last quantities are obtained from numerical fits to the available pre-white dwarf evolutionary sequences and also play a critical role in matching observed white dwarf luminosity functions. The integration limits M_{s} and M_{i} play an important role as well. The upper limit in Eq. (3), is the maximum mass for which a main sequence star is able to produce a white dwarf in its final evolutionary stage. As previously mentioned, this mass is still today somewhat uncertain. Theoretical estimates suggest that its precise value is around $10\,M_{\odot}$ (Ritossa et al., 1999). Finally, the lower limit in Eq. (3) is the minimum mass of a main sequence star able to produce a white dwarf of luminosity L given the total age of the population under study, and it is obtained by solving the following expression:

$$T - t_{\text{cool}}(L, M_{\text{i}}) - t_{\text{MS}}(M_{\text{i}}) = 0, \tag{4}$$

which is to say that the progenitor of the white dwarf was born at $t = 0$. Clearly, as the luminosity decreases the cooling time increases and the net result is that the minimum masses of the main sequence stars able to produce a white dwarf of the appropriate luminosity increase. Thus, M_{i} approaches M_{s} for decreasing luminosities. This produces a down-turn in the theoretical white dwarf luminosity function which can be compared to the observational data, yielding an estimate of the age of the population under study. This has been (and still is) one of the most successful applications of the white dwarf luminosity function.

It is important to realize that the position of the down-turn in the white dwarf luminosity function is totally independent of the initial mass function of the population under study, a fact that makes this method very appealing. Moreover, the position of the down-turn of the white dwarf luminosity function measures the time elapsed since the beginning of *significant star formation activity* in the population under study. Thus, strictly speaking, only lower limits to the age of the population can be retrieved from the white dwarf luminosity function. It should also be noted that the exact shape of the down-turn depends — although weakly — on the adopted star formation rate. Abrupt down-turns occur when constant star formation rates are used, but the slope of the down-turn is shallower for slowly increasing star formation rates. Also, beyond the down-turn, there is a low-luminosity tail which is due to the contribution of massive white dwarfs and/or contamination by much older halo white dwarfs. Hence, the shape of this tail is sensitive to the adopted initial mass function and to the initial-to-final mass relationship. Unfortunately, present white dwarf surveys are not nearly deep enough to reach this population of ultra-low luminosity white dwarfs.

In order to compare to the observations properly, it is usually convenient to bin the theoretical luminosity function in one- or half-magnitude intervals ΔM_{bol}, in the following way:

$$\langle n(L) \rangle_{\Delta M_{\text{bol}}} = \frac{1}{\Delta M_{\text{bol}}} \int_{l-0.5\Delta M_{\text{bol}}}^{l+0.5\Delta M_{\text{bol}}} n(L) \, dM_{\text{bol}} \tag{5}$$

where ΔM_{bol} is the size of bolometric magnitude bin. This procedure introduces additional sources of uncertainty that must be taken into account — see, for example, Butkevich et al. (2005).

24

3.1. Monte Carlo simulations

The procedure previously described is the most straightforward way of constructing the theoretical white dwarf luminosity function. However, there exist alternatives. The key point is that Eq. (3) does not take into account the many subtle selection biases that affect the observational determination of the white dwarf luminosity function from the existing white dwarf catalogs. Monte Carlo techniques help to account for these subtleties. Even though prior Monte Carlo simulators (Wood and Oswalt, 1998; García-Berro et al., 1999; Torres et al., 2001, 2002; García-Berro et al., 2004) adopted very different approaches, they demonstrated useful ways to evaluate biases in the observational data. For instance, Wood and Oswalt (1998) distributed white dwarfs according to a previously computed integrated luminosity function, whereas other Monte Carlo simulators (García-Berro et al., 1999; Torres et al., 2002; García-Berro et al., 2004; Torres et al., 2013) incorporated full models of Galactic structure and evolution. Both approaches are valid and produce reasonable results when all the sample selection procedures and observational biases are taken into account. Using these tools it has been possible to assess the quality of the observational data, the statistical significance of the samples used to obtain the observed white dwarf luminosity function, the sample selection procedures, and the method used to derive the white dwarf luminosity function. We review these results below.

Previous observational efforts, which were described in Sect. 2, have provided an invaluable wealth of good quality data. Moreover, ongoing projects like those detailed in Sect. 7 will undoubtely increase the sample of spectroscopically-identified white dwarfs with reliable determinations of parallaxes and proper motions, which are essential for an accurate determination of the white dwarf luminosity function. Last but not least, future space missions like Gaia (Perryman et al., 2001) will dramatically increase the sample of known white dwarfs with very accurate astrometric data (Jordan, 2007; Jordan and de Bruijne, 2013). However, the rapid increase in both the quality and the quantity of observational data has not been accompanied by corresponding improvements in the way observational data are analyzed. Thus, the main aim of the Monte Carlo simulations performed up to now has been to assess the reliability of the most common method used to estimate the disk white dwarf luminosity function — the $1/\mathcal{V}_{\max}$ method (Schmidt, 1968, 1975b; Felten, 1976) — and to test other techniques which eventually could allow more accurate determinations of the white dwarf luminosity function. Examples of these more sophisticated techniques are, for instance,

the C^- method (Lynden-Bell, 1971), the STY method (Sandage et al., 1979), the Choloniewski method (Choloniewski, 1986), and the Stepwise Maximum Likelihood method (Efstathiou et al., 1988) which, among others, are currently used to derive galaxy luminosity functions.

Two preliminary studies (Wood and Oswalt, 1998; García-Berro et al., 1999) demonstrated — using two independent Monte Carlo simulators — that the $1/\mathcal{V}_{max}$ method for proper-motion selected samples is a good density estimator. However, it is subject to important statistical fluctuations when estimating the slope of the bright end of the white dwarf luminosity function where the space density of stars is low and subject to small number statistical uncertainties. In the latter of these works it was also shown that a bias in the derived ages of the solar neighborhood is present — a consequence of the binning procedure. Additionally, it has been shown (Geijo et al., 2006) that the size of the observational error bars assigned by the $1/\mathcal{V}_{max}$ method is severely underestimated and that more robust luminosity function estimators should be used. These alternative estimators provide a good characterization of the shape of the white dwarf luminosity function even when small numbers of objects are used. Moreover, Geijo et al. (2006) found that for a small sample size the $1/\mathcal{V}_{max}$ method provides a poor characterization of the less populated bins, while for large samples the Choloniewski method and the $1/\mathcal{V}_{max}$ method are comparable. In this case both provide the shape of the disc white dwarf luminosity function and the precise location of the down-turn with reasonable accuracy. This study also showed that a reliable observational white dwarf luminosity function can be best obtained by using a combination of both the $1/\mathcal{V}_{max}$ method and the Choloniewski method, while other parametric maximum-likelihood estimators are not recommended for small sample sizes. These preliminary tests also showed that these sophisticated algorithms work better for larger sample sizes. Undoubtely, with the advent of massive sets of good quality observational data employing these algorithms will be among the priorities of the research field. More recently Torres et al. (2007) have shown that when the sample size is small it might be affected by the Lutz-Kelker bias (Lutz and Kelker, 1973) and that contamination of the disk sample by high–velocity halo white dwarfs can have dramatic effects on the low–luminosity bins. Work in this direction will also be one of the priorities during the next few years.

4. Overview of the white dwarf cooling theory

As mentioned previously, the key ingredient to computed theoretical white dwarf luminosity functions is a detailed description of the cooling process of white dwarfs. In this section we provide an overview of the procedure. The evolution of a carbon-oxygen white dwarf from the planetary nebula phase to its disappearance depends on the properties of the envelope and the core. This process has been discussed in detail in a large number of papers (Iben and Tutukov, 1984; Koester and Schoenberner, 1986; D'Antona and Mazzitelli, 1989; Wood, 1992; Segretain et al., 1994; Benvenuto and Althaus, 1999; Hansen, 1999; Chabrier et al., 2000; Salaris et al., 2000; Fontaine et al., 2001; Prada Moroni and Straniero, 2002) — see also Isern et al. (2013) for a relatively brief review of the cooling theory of carbon-oxygen white dwarfs. The cooling of helium white dwarfs has also received extensive attention (Benvenuto and Althaus, 1998; Hansen and Phinney, 1998; Driebe et al., 1998, 1999; Sarna et al., 2000; Althaus et al., 2001a,b; Serenelli et al., 2001, 2002), whereas the cooling of oxygen-neon white dwarfs has received less attention (Garcia-Berro et al., 1997; Althaus et al., 2005a, 2007). Independently of the chemical composition of the core, the cooling process can be roughly divided into four stages: neutrino cooling, cooling in the fluid phase, crystallization and Debye cooling. We discuss each phase in the following subsections. In what follows the luminosity (instead of the magnitude) will be used to describe these phases, as it is customary in the field. To ease the comparison with observational studies we remind the reader that the absolute magnitude and the luminosity of the white dwarf are related by the well-known expression $M_v = -2.5 \log(L/L_\odot) + 4.74 + \text{B.C.}$, where B.C. is the bolometric correction that accounts for the portion of the star's spectral energy distribution that does not pass through the V filter (Allen, 1973).

4.1. The cooling phases

The first evolutionary phase of typical white dwarfs is dominated by neutrino cooling. This phase occurs for $\log(L/L_\odot) \gtrsim -1.2$. It is rather complicated because the initial conditions of the star and the behavior of the envelope are still not yet fully understood. For instance, if the thickness of the hydrogen layer is large enough the luminosity due to hydrogen burning through the pp-chain may never stop and could become dominant at low luminosities, i.e., $-3.5 \lesssim \log(L/L_\odot) \lesssim -1.5$ (Iben and Tutukov, 1984). In this case the cooling rate would be similar to that obtained ignoring this

source of energy, and it would be observationally impossible to distinguish between the two. However, the importance of continued H-burning strongly depends on the mass, $M_{\rm H}$, of the hydrogen layer. If $M_{\rm H} \leq 10^{-4} \, M_{\odot}$, the pp contribution quickly drops and never becomes dominant, except for low-mass, low-metallicity white dwarfs (Miller Bertolami et al., 2013; Althaus et al., 2015). Since astero-seismological observations seem to constrain the size of $M_{\rm H}$ well below this critical value, this source can be neglected. Fortunately, when neutrino emission becomes dominant, the different thermal structures converge to a unique solution, assuring the uniformity of models with $\log(L/L_{\odot}) \lesssim -1.5$. Furthermore, since the time necessary to reach this value is $\lesssim 8 \times 10^7$ years for any model (D'Antona and Mazzitelli, 1989), its influence in the total cooling time is negligible.

After the neutrino cooling phase the core of the white dwarf is liquid. This stage occurs for luminosities in the range $-1.5 \gtrsim \log(L/L_{\odot}) \gtrsim -3$. Here gravothermal energy becomes dominant. Since the plasma is not very strongly coupled, its properties are reasonably well known (Segretain et al., 1994). To characterize the properties of the plasma it is customary to define the Coulomb coupling parameter

$$\Gamma = \langle Z^{5/3} \rangle \Gamma_{\rm e} \tag{6}$$

where

$$\Gamma_{\rm e} = \frac{e^2}{a_{\rm e} k_{\rm B} T}, \tag{7}$$

Z is the atomic charge, $a_{\rm e}$ is the inter-electronic distance, $k_{\rm B}$ is the Boltzmann constant, e is the electron charge, and T is the temperature. This phase is characterized by small Coulomb coupling parameters, $\Gamma < 179$. During this phase the observed luminosity is controlled by a thick non-degenerate layer with an opacity dominated by hydrogen (if present) and helium, and it is weakly dependent on the metal content. The main source of uncertainty is related to the chemical structure of the interior, which depends on the rather uncertain adopted rate of the $^{12}{\rm C}(\alpha, \gamma)^{16}{\rm O}$ reaction and on the treatment given to semiconvection and overshooting during the pre-white dwarf evolutionary phases. If this rate is high, the oxygen abundance is higher in the center than in the outer layers. This results in a reduction of the specific heat at the central layers where the oxygen abundance can reach values as high as $X_{\rm O} = 0.85$ (Salaris et al., 1997).

When the Coulomb coupling parameter reaches a critical value, $\Gamma \simeq 179$, crystallization at the center of the white dwarf sets in, and a new cooling phase starts, as early recognized by Kirshnitz (1960), Abrikosov (1961), and Salpeter (1961). Crystallization leads to the release of latent heat, which then controls the evolution of white dwarfs (van Horn, 1968; Lamb and van Horn, 1975), and to the release of gravitational energy due to phase separation. The typical luminosities during this phase are $\log(L/L_\odot) \lesssim -3$. The release of gravitational energy associated with changes in the chemical composition induced by crystallization in carbon-oxygen mixtures has been examined by Stevenson (1980); Mochkovitch (1983); Althaus et al. (2012). Finally, the consequences of the deposition of ^{22}Ne, the most abundant of the impurities present in the central regions of a white dwarf have been examined (Isern et al., 1991). A similar calculation for ^{56}Fe, the second most important impurity, was made somewhat later (Xu and van Horn, 1992). We elaborate on this below, in Sect. 4.3. Crystallization introduces two new sources of energy: latent heat and sedimentation (a form of gravitational energy release). In the case of Coulomb plasmas, the latent heat is small, of the order of $k_B T_s$ per nucleon, where T_s is the temperature of solidification. Its contribution to the total luminosity is small, $\sim 5\%$, but not negligible (Shaviv and Kovetz, 1976).

During the crystallization process, the equilibrium chemical compositions of the solid and liquid plasmas are not equal. Therefore, if the resulting solid flakes are denser than the liquid mixture, they sink towards the central regions. If they are lighter, they rise upwards and melt when the solidification temperature, which depends on the density, becomes equal to that of the isothermal core. The net effect is a migration of the heavier elements towards the central regions with the subsequent release of gravitational energy Mochkovitch (1983). The efficiency of the process depends on the detailed chemical composition and on the initial chemical profile. It is most efficient in a mixture made of half oxygen and half carbon uniformly distributed throughout the star.

The first calculation of a phase diagram for C/O mixtures yielded an eutectic shape (Stevenson, 1980), denoting a mixture of elements in fixed proportions that solidifies and melts at a given temperature that is lower than the melting points of either constituent or different mixture. This resulted from the assumption that the solid was entirely random, so that the free energy is given by $F \sim -0.9\Gamma$ (Segretain et al., 1994), where Γ is defined by Eq. (6) . Since the mixture retains some short range order, the free en-

ergy is then given by the linear mixing rule, $F_{lm} \sim -0.9\langle Z^{5/3}\rangle\Gamma_e$. The solid phase is less stable, and thus $F > F_{lm}$, resulting in an eutectic behavior of the phase diagram. The density functional theory of freezing and the mean spherical approximation, but with the same diameter for the two chemical species, were used later to compute the correlation between the particles, and a phase diagram of spindle form was obtained (Barrat et al., 1988). A similar calculation in the framework of the density functional theory, but using the Improved Hypernetted Chain approximation to compute the correlation functions, was performed, producing an azeotropic phase diagram (Ichimaru et al., 1988), indicating a mixture of liquids whose proportions are not affected by a phase change. Finally, these calculations were extended to include the effects of the different diameters of the two chemical species (Segretain and Chabrier, 1993) and the same results of Barrat et al. (1988) were found. More recently, Horowitz et al. (2010) computed a new phase diagram for the C/O mixture using an advanced technique, direct molecular dynamics, again agreeing with previous results, thus settling this issue.

The so-called Debye cooling phase comes last. It occurs at small luminosities, typically $\log(L/L_\odot) \lesssim -4.5$, when the star is almost entirely crystallized. During this cooling phase for a large fraction of the crystallized core the specific heat follows Debye's law, and scales as T^3. Due to the reduced specific heat, cooling accelerates and the star's luminosity drops abruptly. However, the outer layers still have very large temperatures relative to the Debye temperature, and since their total heat capacity is still large enough, they prevent the sudden disappearance of the white dwarf, at least when the envelope is thick (D'Antona and Mazzitelli, 1989).

4.2. The opacity of the envelope

The importance of the atmospheric treatment in the cooling models for white dwarfs cannot be overstated. In the strongly degenerate core energy transfer by electron conduction dominates. This has been shown to be a very efficient mechanism. Thus, the cores of white dwarfs are essentially isothermal. However, in the outer layers radiation and, depending on the effective temperature, convection dominates the energy transfer. In these layers the temperature profile is determined by the equation of state. Thus, changes in atmospheric parameters directly affect the core temperature and, since white dwarf cooling is driven largely by the slow leakage of the thermal reservoir stored in the core, it moderates the cooling rate. Until recently the atmospheric treatment was based on grey atmospheres and Rosseland mean

opacities. Modern calculations incorporate detailed non-grey atmospheres. Recall that at low effective temperatures, collision-induced absorption by molecular hydrogen due to collisions with H_2 represents a major source of opacity in the infrared and dominates the shape of the emergent spectrum. Thus, very cool white dwarfs with hydrogen-dominated atmospheres begin to turn blue at about 4,500 K, whereas helium-dominated atmospheres resemble black bodies (Hansen, 1998; Saumon and Jacobson, 1999; Rohrmann, 2001). The cooling rate, in both cases, depends sensitively on the adopted mass and composition of the envelope, and the age differences are substantial, larger than 1.5 Gyr, at the relevant luminosities, $\log(L/L_\odot) \lesssim -4.5$ (Hansen, 1998).

We note here that for all the cooling phases described in the previous section the importance of the envelope is crucial for two reasons. Clearly, more transparent envelopes result in faster energy losses and shorter cooling times. This is true for all the previously listed cooling phases. The second reason is more subtle and was largely overlooked until some time ago (Fontaine et al., 2001), but it is essential to take into account during the crystallization phase. Theoretical calculations predict that at approximately the same evolutionary stage in which crystallization sets in, the external convection zone penetrates the region where thermal conduction by degenerate electrons is very efficient. Such an occurrence (known as convective coupling), initially produces a further decrease in the cooling rate, followed by a more rapid decline. In fact, it has been proven that the delay introduced by the convective coupling can be as large as that produced by chemical differentiation during crystallization (Fontaine et al., 2001).

4.3. The role of minor chemical species

Minor chemical species like ^{22}Ne or ^{56}Fe can also play an important role in the cooling of white dwarfs. These minor chemical species are the products of the pre-white dwarf evolutionary stages. The most abundant is ^{22}Ne. Its abundance is directly related to the initial abundances of CNO elements, which, after the H-burning phase become ^{14}N. This isotope, in turn, becomes ^{22}Ne after the series of reactions $^{14}N(\alpha, \gamma)^{18}O(\alpha, \gamma)^{22}Ne$, during the He-burning phase. Because of its large neutron number and the high sensitivity of degenerate structures to the electron number profile, ^{22}Ne can induce a large release of gravitational energy if, as a consequence of crystallization, it migrates towards the center during crystallization (Isern et al., 1991). For stars of solar metallicity, the typical abundances are 1–2%. A similar effect

31

can be produced by the deposition of ^{56}Fe at the center (Xu and van Horn, 1992). In this case, typical abundances are 0.1%.

The physics of the deposition of the minor species is intricate since it depends on the behavior of a multicomponent phase diagram that is not yet known. A first step consists in assuming that the C/O/Ne or C/O/Fe mixtures behave as an effective binary mixture composed of neon (or iron) and an average element, representative of the C/O mixture. The phase diagram for arbitrary ionic mixtures as a function of the charge ratio has been computed by Segretain and Chabrier (1993). It was found that the phase diagram is of the spindle form for $0.72 \lesssim Z_1/Z_2 < 1$, of the azeotropic form for $0.58 \lesssim Z_1/Z_2 \lesssim 0.72$ and of the eutectic form for $Z_1/Z_2 \lesssim 0.58$. In the case of a C/O mixture made of equal mass fractions of carbon and oxygen, the resulting average element has such a charge that the corresponding phase diagram shows an azeotropic behavior with an azeotropic abundance of $X_a = 0.16$. This means that white dwarfs are in the neon-poor side of the phase diagram. Consequently, the solid in equilibrium with the liquid has a smaller concentration of neon and, since it is lighter than the surrounding liquid, it will rise and melt in lower density regions so that the neon concentration in the liquid will increase until it reaches the azeotropic composition. This process will continue until all ^{22}Ne is collected in a central sphere of mass $M_{WD}X_0(Ne)/X_a(Ne)$. Following the procedure described in Isern et al. (1997) for computing the decrease in the cooling rates suggests that the total energy release in the case of ^{22}Ne is $\Delta E \simeq 1.52 \times 10^{47}$ erg for a typical $0.6\,M_\odot$ white dwarf. At the corresponding luminosity, this would result in an unrealistic delay of about 9 Gyr, indicating that there is a problem with the adopted assumptions. For the case of ^{56}Fe under the same conditions the energy released is much smaller, $\Delta E \simeq 2.0 \times 10^{46}$ erg, and thus the resulting time delay is also much smaller, $\Delta t \simeq 1.1$ Gyr.

The assumption of an effective binary mixture of the C/O/Ne mixture is probably not very realistic. In fact, a preliminary ternary diagram has been computed for the C/O/Ne mixture (Segretain, 1996). This phase diagram displays the expected behavior at the binary limit (spindle form for the C/O mixture, azeotropic form for the C/Ne mixture and spindle form for the O/Ne mixture). For small concentrations of neon, of the order of a few percent, and temperatures well above the azeotropic temperature, the crystallization diagram is not influenced by the presence of neon. However, as the temperature approaches the azeotrope, the resulting solid is lighter than the surrounding liquid and the distillation process starts as in the previous

case. The main difference is that it starts in the outer layers instead of the central layers and the effect of separation is therefore much smaller. As a matter of fact, the total energy released in this case is $\Delta E \simeq 0.20 \times 10^{46}$ erg and the corresponding effect on the cooling times are hence much smaller, of the order of 0.6 Gyr.

Up to this moment we have reviewed the role played by the impurities in the cooling of white dwarfs during the crystallizing phase. However, it is important to realize that ^{22}Ne can also play an important role during the liquid cooling phase. Building on earlier work (Bravo et al., 1992) it has been recently shown (Bildsten and Hall, 2001; Deloye and Bildsten, 2002; Althaus et al., 2008, 2010b) that due to the large neutron excess of ^{22}Ne it sinks towards the interior as the liquid white dwarf cools. The subsequent gravitational energy released slows the cooling of the white dwarf by 0.25–1.6 Gyr by the time it has completely crystallized, depending on the white dwarf mass and on the adopted sedimentation rate. This effect will make massive white dwarfs or those in metal-rich clusters appear younger than their true age. It has been demonstrated (García-Berro et al., 2010) that this is indeed the case, and that the slowdown of the white dwarf cooling rate owing to the release of gravitational energy from ^{22}Ne sedimentation and carbon-oxygen phase separation upon crystallization is of fundamental importance to reconcile the age discrepancy of the very old, metal-rich open cluster NGC 6791. Nevertheless, although the white dwarf luminosity function of this open cluster provides a statistical measure, a direct test remains to be done. Since there is no way to measure the metallicity of single white dwarf progenitors we would need a wide binary composed of a non-evolved star and a white dwarf, for which we could accurately measure the age and metallicity using independent methods (Zhao et al., 2012).

4.4. Uncertainties in the cooling ages

Table 1 displays the uncertainties in the time necessary for a typical white dwarf of 0.6 $M_\odot$ to reach a luminosity of $\log(L/L_\odot) = -4.5$. In the bottom section of this table the additive contributions to the uncertainty due to the physics of crystallization are shown, whereas the top section describes the uncertainties due to the rest of the input physics. The major contribution is provided by the minor chemical species and all contributions are of the same order of magnitude, ~ 1 Gyr. The largest contributions come from the core composition and the conductive opacities (Prada Moroni and Straniero, 2002, 2007). Also the adopted composition of the envelope has an important

Table 1: Uncertainties in the estimates of the cooling time of white dwarfs.

Input	Δt (Gyr)	Comments
Core composition	$\lesssim 0.6$	Depending on the $^{12}C(\alpha,\gamma)^{16}O$
Opacity	$\lesssim 0.4$	
Conductive opacity	$\lesssim 1.0$	
Metals in the envelope	≈ 0.2	
Metallicity of the progenitor	$\lesssim 0.2$	
Additive contributions of the crystallization process		
C/O	0.8–1.2	Depending on the $^{12}C(\alpha,\gamma)^{16}O$
Fe	$\lesssim 1.3$	
Ne	$\lesssim 0.5$	Ternary mixture
Observational	1–2	

influence on age estimates for a white dwarf population, although hydrogen-rich cooling sequences are usually adopted, as most observational determinations of the white dwarf luminosity function rely on the population of DA white dwarfs.

There is, however, another point of concern, namely how the different numerical implementations of the evolutionary codes affect the accuracy of the cooling times. This issue has been examined by Salaris et al. (2013). These authors compare the cooling ages obtained using a set of controlled input physics and very different numerical schemes. This comparison shows that when the same physical inputs are adopted the cooling ages do not differ by more than a very modest $\sim 2\%$ at all luminosities, in sharp contrast with main sequence ages, for which the typical differences are of the order of $\sim 6\%$, or even larger. This difference is smaller than the uncertainties in cooling times attributable to the present uncertainties in the white dwarf chemical stratification. Hence, white dwarf cooling ages turn out to be even more robust than main sequence evolutionary ages.

5. Other key ingredients

In this section we discuss the other main quantities needed to compute theoretical white dwarf luminosity functions. In particular, we discuss the appropriate choice of an initial-to-final mass relationship, which main sequence lifetimes can be used to calculate luminosity functions, which initial mass

functions are usually employed in the theoretical calculations, and finally, we also provide a preliminary discussion of the role of the star formation rate.

5.1. Initial-to-final mass relationship

One of the key ingredients of a theoretical white dwarf luminosity functions is a relationship linking the mass of the white dwarf and that of its progenitor at the zero age main sequence. It is well known that theoretical evolutionary calculations predict a positive correlation between both quantities. However, the precise shape of the initial-to-final mass relationship is troublesome to predict on theoretical grounds alone. This is a consequence of the intrinsic difficulties associated with modeling several complex physical phenomena involved in the final phases of stellar evolution. A number of theoretical works have attempted to address these issues (Domínguez et al., 1999; Girardi et al., 2000; Marigo, 2001; Karakas et al., 2002; Marigo and Girardi, 2007; Salaris et al., 2009; Renedo et al., 2010), but the area is an ongoing active field of research, and remains open. In general, the theoretical predictions depend sensitively on many subtle details of the evolutionary codes (Weidemann, 2000b). However, there is a general consensus that this relationship is almost linear for progenitor masses between $\simeq 1.2$ and $6.5\,M_\odot$ (Kalirai et al., 2008; Catalán et al., 2008b,a; Casewell et al., 2009), although there are indications that the slope becomes steeper for masses larger than roughly $3.5\,M_\odot$ (Dobbie et al., 2009). The question of whether this relationship depends on the metallicity of the population under study remains controversial — see, for instance Althaus et al. (2015), and references therein.

Much effort has been invested in empirically determining the slope of the initial-to-final mass relationship. This is usually done by employing either open clusters or detached, non-interacting binaries composed of a white dwarf and a main sequence star. The best-studied systems of the latter kind are common proper motion pairs. For these binaries we are confident that both stars are physically associated. In both cases we know the total age, and hence the total age of a given white dwarf (cooling age plus the lifetime of its progenitor). This allows determination of the mass of its progenitor, once the mass of the white dwarf is measured, provided that an accurate relationship between the mass and the main sequence lifetime is available — that is, a set of reliable isochrones. The main drawback of employing open clusters for this task is that well-populated clusters are needed. Additionally, since usually open clusters are young, they only probe a limited range of masses, between 2.5 and $7.0\,M_\odot$, an interval corresponding to the most massive white

dwarfs. Moreover, open clusters often show a metallicity spread, and the information about the metallicity of the progenitor of the white dwarf is lost once the star becomes a white dwarf. This, in turn, introduces an uncertainty. Weidemann (1977) pioneered the observational efforts to empirically determine the initial-to-final mass relationship using open clusters, studying white dwarfs in Hyades and Pleiades. Following this early work several other clusters were studied (Weidemann, 1987, 2000b; Ferrario et al., 2005; Dobbie et al., 2006; Kalirai et al., 2008; Rubin et al., 2008; Casewell et al., 2009; Dobbie et al., 2009; Williams et al., 2009), and it is expected that this work will be extended to fainter and older clusters in the coming years.

Common proper motion pairs (Wegner, 1973; Oswalt et al., 1988) provide a work-around for most of these concerns. In such binaries the stars have never interacted and both components evolve as single stars. As they were born simultaneously, the total age of the white dwarf can be split into its cooling age and that of its progenitor star. The age of the companion star (hence, the total age of the binary system) is measured using an independent method, for example a set of theoretical isochrones of the appropriate metallicity, from rotation rate, or from chromospheric activity. The main inconvenience of this method is that reliable age determinations are available for only a handful of binary systems (Catalán et al., 2008b,a; Zhao et al., 2012).

A third method, though less frequently employed, to determine the shape of the initial-to-final mass relationship is to calculate the difference of cooling times between two white dwarfs in a double degenerate system (Finley and Koester, 1997). Until recently this method was hampered by the small number of such systems known. Andrews et al. (2015) identified new candidate double degenerates in the SDSS, bringing the total known to 142. For over 50 systems, they were able to derive masses and cooling ages from Balmer line spectra and employed a Bayesian statistical approach to fitting the most probable initial-to-final mass ratio consistent with the sample for initial masses of $2 - 4\,M_\odot$. Open clusters provide little leverage within this mass range, so double degenerates provide a valuable alternative approach. Since these methods make use of both observed data and theoretical models the results are known as semi-empirical initial-to-final mass relationships.

In any case, there are two options to compute theoretical white dwarf luminosity functions. Either semi-empirical, or theoretical initial-to-final mass relationships can be employed. In general, most theoretical calculations of the luminosity function of disk white dwarfs are done using semi-empirical re-

lationships, whereas when luminosity functions of stellar systems with known metallicity are computed theoretical initial-to-final mass relationships of the appropriate metallicity are employed. This includes the calculation of white dwarf luminosity functions for the Galactic halo, or for open and globular clusters in the Galaxy.

5.2. Main sequence lifetimes

Main sequence lifetimes are also necessary to theoretically derive white dwarf luminosity functions — see Eq. (3). Ideally, one should use main sequence lifetimes consistent with the adopted initial-to-final mass relationship. However, this is not always possible. Hence, many calculations employ a simple relationship between the mass of the progenitor of a white dwarf at the zero age main sequence and its lifetime. An example of this simple relationship is that of Iben and Laughlin (1989):

$$t_{\mathrm{MS}} = 10^{10} \left(\frac{M}{M_\odot} \right)^{-3.5} \mathrm{yr} \tag{8}$$

However, there are more sophisticated treatments, which include the use of interpolation in theoretical isochrones. An example of such more elaborated treatments consists in interpolating within the BaSTI isochrones[1] for the appropriate metallicity of the white dwarf progenitor (Pietrinferni et al., 2004).

5.3. The initial mass function

Another, less relevant but necessary, input to compute theoretical white dwarf luminosity functions is the initial mass function. This function peaks at a few tenths of a solar mass, and shows an extended tail for masses larger than this value. It is customary to model this tail as a power law, with a fixed exponent, or in some cases as a combination of power laws, again with fixed exponents. A thorough discussion of the initial mass function is far beyond the scope of this work, but the interested reader will find useful the excellent review of Kroupa (2002). As a matter of fact, most studies employ the classical Salpeter-like initial mass function (Salpeter, 1955), which is a power law with just one index α. That is, $\Phi(M) \propto M^{-\alpha}$, where M is the mass at the zero age main sequence. In some cases the power-law

---

[1]http://albione.oa-teramo.inaf.it/

index is considered a free parameter to fit the observations. However, more sophisticated studies prefer to employ the so-called "universal" mass function of Kroupa (2001) — which for the mass range relevant to most stellar systems is totally equivalent to a two-branch power law with exponent $-\alpha$, with $\alpha = 1.3$ for $0.08 \leq M/M_\odot < 0.5$ and $\alpha = 2.30$ for $M/M_\odot \geq 0.5$. Finally, sometimes a top-heavy initial mass function:

$$\Phi(M) = \frac{1}{M} \exp\left(\frac{-\log(M/\mu)}{2\sigma^2}\right) \tag{9}$$

is adopted. In this expression $\mu = 10\,M_\odot$ and $\sigma = 0.44$. This initial mass function was introduced by Suda et al. (2013), and is dominated by high mass stars. It has been found that this function better reproduces the characteristics of metal-poor populations, namely those with [Fe/H]≤ -2.

5.4. The star formation rate

The final ingredient in the calculation of a theoretical white dwarf luminosity function is the star formation rate. The star formation rate depends on the characteristics of the population under study. For the case of the disk white dwarf population a constant star formation rate is usually adopted, whereas for metal-poor populations — namely the stellar spheroid and the system of globular clusters — a short, intense burst of star formation is adopted. Typically, the duration of the burst is a free parameter that can be used to better fit the observed white dwarf luminosity function and the color distribution. In fact, if all the ingredients to model the white dwarf luminosity function are known with good accuracy one could eventually use Eq. 3 to solve the inverse problem and derive the star formation history of the population under study. Unfortunately, this is not usually possible, and moreover, the solution of the inverse problem does not have a unique solution. We elaborate on this in Sect. 6.2.

6. Applications of the white dwarf luminosity function

6.1. The white dwarf population and the age of the Galaxy

As mentioned above, the potential use of white dwarf stars as chronometers was recognized several decades ago (Schmidt, 1959), but only in the last two decades has there been good observational data and reliable theoretical cooling sequences which are necessary to interpret them in terms of an age for

the Galactic disk. A determination from the white dwarf luminosity function of the age of the halo population still remains to be done, due to the scarcity of halo white dwarfs in the solar neighborhood.

The evidence for a decrease in the number counts of white dwarfs at lower luminosities was suspected but unobtainable until larger telescopes with more quantum efficient detectors were applied to systematic surveys for white dwarfs. In fact, the early white dwarf luminosity functions were constrained by the available data, and only the bright portion of the luminosity function — namely, those bins with $\log(L/L_\odot) \lesssim -3.5$ — had reliable determinations. However, the improved observational efforts resulted in the first convincing identification of a down-turn in the disk white dwarf luminosity function (Liebert et al., 1988), which was interpreted as a consequence of the finite Galactic age (Winget et al., 1987). This discovery was followed by a series of papers in which progressively more sophisticated cooling sequences, observing strategies and analysis techniques were employed (Garcia-Berro et al., 1988; Wood, 1992; Hernanz et al., 1994; Oswalt et al., 1996; Garcia-Berro et al., 1996; Bergeron et al., 1997; Richer et al., 2000).

The effect of the white dwarf initial-to-final mass relation on the luminosity function has been examined by Catalán et al. (2008a). Fitting theoretical luminosity functions from a variety of stellar evolutionary inputs to the average of the observed luminosity functions of Liebert et al. (1988), Oswalt et al. (1996), Leggett et al. (1998), and Knox et al. (1999), it was shown that the only significant difference between the theoretical fits occurs beyond the down-turn in the luminosity function, where current data is sparse. They also found that a disk age of ~ 11 Gyr consistently fit their composite observed luminosity function best, a value that is substantially older than prior determinations. At present there does not appear to be a generally-accepted age for the Galactic disk derived from the white dwarf luminosity function — it should still be regarded as a work in progress because of the difficulty in obtaining a statistically significant sample of stars in the most important faintest luminosity bins as well as remaining uncertainties in core composition and atmospheric opacities in the coolest white dwarfs. However, a rough average derived from the references discussed in this review — see Table 2 — suggests that star formation in the solar neighborhood (thin disk) began about 10 Gyr ago. This estimate is uncertain by at least ten percent.

Finally, it is worth emphasizing that the age estimates obtained using the down-turn in the disk white dwarf luminosity function, regardless of

the observed sample, are very robust lower limits. As mentioned earlier, the white cooling ages obtained employing different numerical evolutionary codes differ by only a few percent when a standard set of physical assumptions is adopted, a quite remarkable feature. Not only that, it has been recently demonstrated (Cojocaru et al., 2014) that the age estimates of the Solar neighborhood obtained by fitting the position of the down-turn in the disk white dwarf luminosity function do not depend on the adopted metallicity law, also ensuring the age determined in this way very reliable. However, a study of super-solar metallicity stars, [M/H] > +0.1 dex, by Kordopatis et al. (2015) employing data from the RAdial Velocity Experiment (RAVE) DR4 suggests that the angular momentum of numerous stars have been increased by scattering at corotation resonance of the Galaxy's spiral arms from regions well within the Sun's Galactocentric radius. This may have ramifications for the local white dwarf luminosity function that remain to be explored.

One would expect the age of the halo derived from the white dwarf luminosity function to be more uncertain than that obtained for the disk, primarily because the halo component is older and comprises at most a few percent of the local white dwarf population. Thus, the typical halo white dwarf is distant and faint. However, based on the handful of currently available studies of the halo white dwarfs in the solar neighborhood and in nearby globular clusters (see Table 2) it can be said that star formation began in that population subgroup at least 11 Gyr ago.

6.2. The star formation history of the Galaxy

In addition to an absolute age for the Galactic disk and space density of white dwarfs, the white dwarf luminosity function also contains information about the star formation and death rates over the history of the Galaxy. However, it is important to note that because cool white dwarfs have very long evolutionary time scales, the past Galactic star formation rate influences the shape of the low luminosity portion of the white dwarf luminosity function. Also, due to the extremely long main sequence lifetimes of low mass stars, which are the progenitors of bright white dwarfs, the shape of the hot branch of the white dwarf luminosity function is also sensitive to the past star formation activity. All this implies that the past star formation activity is still influencing the present white dwarf birthrate and that the past star formation rate could be retrieved from the white dwarf luminosity function, as clearly seen in Eq. (3). Provided that we have a reliable determination of the white dwarf luminosity function and accurate cooling

models, the star formation rate, $\Psi(t)$, can be obtained by solving an inverse problem. This has not been possible yet due in part to the discrepancies between the different observational determinations of the white dwarf luminosity function and also to the still relatively large error bars in each bin. In addition, from the theoretical point of view, the inverse transformation cannot be easily done because the kernel of the transformation is complicated and, more importantly, it is not symmetric. These are the reasons why very few papers have explored the possibility of doing some sort of Galactic archaelogy using the luminosity function of white dwarfs as a tracer of the star formation activity. However, this situation may be improving — see, for example, Rowell and Hambly (2011).

In order to overcome these difficulties, several possibilities have been suggested. The first and most straightforward method requires *a priori* knowledge of the shape of the star formation history and consists of adopting a trial function that depends on several parameters, followed by a search for the values of these parameters that best fit the observed luminosity function. This is accomplished by minimizing the differences between the observed and computed luminosity functions (Yuan, 1989; Noh and Scalo, 1990; Isern et al., 1995, 2001). The second possibility consists of computing the luminosity function for massive white dwarfs (Diaz-Pinto et al., 1994), which have negligible main sequence lifetimes, thus making much easier the solution of the inverse problem. Unfortunately, such white dwarfs are rare. Also, if a significant fraction of massive white dwarfs results from double white dwarf mergers, the problem becomes more complicated, as the method relies on the assumption that white dwarfs with moderately high masses (say between 0.8 and 1.1 $M_\odot$) are the result of single star evolution. Finally, Rowell (2013) presented recently an algorithm for inverting the white dwarf luminosity function to obtain a maximum likelihood estimate of the star formation rate in the solar neighborhood. As expected from the discussion above, the results were found to be most sensitive to the choice of white dwarf cooling models. Use of the algorithm on two independent determinations of the white dwarf luminosity function gave similar results: a bimodal star formation rate with broad peaks 2–3 Gyr and 7–9 Gyr before the present, with star formation commencing about 8–10 Gyr ago. Tremblay et al. (2014) employed individual white dwarf atmosphere models and a complete volume-limited "20 parsec sample" to investigate the local star formation history in the Solar neighborhood and concluded that an enhancement in star formation rate (and consequent increase in white dwarf space density) occurred within the

past 5 Gyr, enhancing the space density of white dwarfs by a factor of ~ 2.5. This roughly agrees with a peak reported by Rowell (2013).

Several attempts have been made to discern structure in observed luminosity functions. An early study (Noh and Scalo, 1990) modeled the effect that various bursts of star formation would have on the white dwarf luminosity function and suggested a modest bump noted by Liebert et al. (1988) might be evidence for such an event about 0.3 Gyr ago. The impact of merger episodes in the Galactic disk on the white dwarf population was examined by Torres et al. (2001) using a Monte Carlo simulator. This study concluded that only relatively small merger episodes involving a few percent or less of the current disk population white dwarfs are compatible with the current kinematics of known white dwarfs and that the white dwarf luminosity function is insensitive to such events. More recently, attention has been called to a plateau in the white dwarf luminosity function obtained from the Sloan Digital Sky Survey near $M_{\mathrm{bol}} = 10.5$ (Harris et al., 2006) — see Figure 1. This luminosity corresponds to a cooling time of 0.3 Gyr. Adding the main-sequence lifetime of 2.5 Gyr for the typical progenitor suggests that a drop in star formation rate may have occurred about 3 Gyr ago after a burst or long duration of higher rate of star formation. So far, not much other work appears to have been attempted in this area, probably because until very recently the sample size of white dwarfs have been small enough that statistical uncertainties dominate the luminosity bins. However, there is reason to be hopeful, because much larger samples of white dwarfs are becoming available.

Of particular interest are the delays between the onset of star formation in the thin disk, thick disk and halo. However, a few caveats are in order. Some of these include possible changes in the initial mass function (Adams and Laughlin, 1996; Gibson and Mould, 1997; Brocato et al., 1999), uncertainties in white dwarf core composition and chemical profile (Isern et al., 1997; Salaris et al., 1997; Panei et al., 2000), phase separation (Isern et al., 1997; Montgomery et al., 1999), incompleteness of the sample (Méndez and Ruiz, 2001; Holberg et al., 2002), unresolved binary star fraction (Liebert et al., 2005; Farihi et al., 2005) and statistical limitations of the method chosen to construct the white dwarf luminosity function (García-Berro et al., 1999; Geijo et al., 2006).

A number of studies have been published which attempted to determine the properties of the halo (Mochkovitch et al., 1990; Tamanaha et al., 1990; Isern et al., 1998b). It is important to realize that the halo white dwarf

luminosity function not only carries information about the age of the halo but also — under certain circumstances — about the initial mass function of the halo. If, as generally accepted, the halo was formed in a very short time scale the halo star formation rate can be well approximated by a burst of negligible duration and the calculation of the integral of Eq. (3) can be simplified, since for all halo white dwarfs we have

$$T = t_{\mathrm{MS}}(M) + t_{\mathrm{cool}}(l, M) \tag{10}$$

In this scenario, each luminosity corresponds to a given mass of the white dwarf progenitor. In other words, the halo white dwarf luminosity function maps the mass of the progenitor of the white dwarf as a function of the luminosity, $M = M(l)$. Taking into account that the white dwarf luminosity function is the number of white dwarfs per unit bolometric magnitude, $n(l) \propto dN/dl$, we have:

$$n(l) \propto \frac{dN}{dl} = \frac{dN}{dM}\frac{dM}{dl} = \Phi(M)\frac{dM}{dl} \tag{11}$$

Thus, once we have complete samples of the halo white dwarf population and reliable observational determinations of the halo white dwarf luminosity function, the initial mass function of the halo can be experimentally obtained. This assumes, of course, that we have accurate and precise white dwarf cooling sequences. Another concern is that the initial-to-final mass relation for white dwarfs could depend upon the metallicity of their main sequence progenitors — see Zhao et al. (2012). The expectation is that low metallicity halo white dwarfs are born with thicker hydrogen envelopes, leading to more prolonged shell burning than in disc white dwarfs. In addition, stars of higher primordial metallicity are expected to be more efficient in shedding mass during the AGB phase, resulting in lower mass white dwarfs. Consequently, this could affect the white dwarf luminosity function and its interpretation for different populations (Miller Bertolami et al., 2013; Althaus et al., 2015). Fortunately, the most recent work on this problem suggests that the shape of the white dwarf luminosity function from bright to faint bin is relatively insensitive to metallicity (Cojocaru et al., 2014).

6.3. Other applications

Other applications of the white dwarf luminosity function include independent constraints on the physical mechanisms operating during the cooling

process, an independent test of the constancy of the gravitational constant, G, and its use as an astro-particle physics laboratory. We examine all three below.

As shown previously, the white dwarf luminosity function carries important information about the physics of cooling. Consequently, a reliable white dwarf luminosity function would allow us to test both the mechanisms operating at high effective temperatures — basically neutrino cooling — and the mechanisms which are dominant for relatively low core temperatures (crystallization). Neutrinos are the dominant form of energy loss in model white dwarf stars down to $\log(L/L_\odot) \simeq -2.0$, depending on the stellar mass. Consequently, the evolutionary timescales of white dwarfs at these luminosities sensitively depend on the ratio of the neutrino energy loss to the photon energy loss. Thus, the slope of the bright end of the white dwarf luminosity function directly reflects the importance of neutrino emission. Although the unified electroweak theory of lepton interactions that is crucial for understanding neutrino production has been well tested in the high-energy regime — see, for instance, Hollik (1997) for an excellent review — the white dwarf luminosity function could help to test the low-energy regime of the theory (Winget et al., 2004; Torres et al., 2005). For example, recent work by Miller Bertolami (2014) using the best available white dwarf luminosity functions and including the effects of observational errors and binning have set a firm limit on the neutrino magnetic dipole moment; $\mu_\nu < 5 \times 10^{-12} e\hbar/(2m_\mathrm{e}c)$. This is comparable to the constraints on μ_ν set by studies of globular clusters.

The white dwarf luminosity function can also put constraints on the physical mechanisms that operate at low core temperatures, namely crystallization and phase separation. As discussed previously, the inclusion of phase separation upon crystallization in the cooling sequences adds an additional delay to the cooling (and, thus, considerably modifies the characteristic cooling times at low luminosities), which depends on the initial chemical profile (the ratio of carbon to oxygen) and on the transparency of the insulating envelope. Thus, if a direct measure of the disk age with reasonable precision is obtained by an independent method, say via main sequence turn-off stars, the white dwarf luminosity function directly probes the physics of crystallization. It is worth noting as well that not only the exact location of the down-turn of the disk white dwarf luminosity function is affected by the details of the cooling sequences but also the position and the shape of the maximum of the white dwarf luminosity function. Thus, additional tests are possible.

A second application of the white dwarf luminosity function involves set-

ting constraints on a hypothetical variation of the gravitational constant, G. There are two reasons for this. First, when white dwarfs are cool enough, their energy is entirely of gravitational and thermal origin, and any change in the value of G modifies the energy balance. This in turn translates into a change of luminosity. Second, since they are long-lived objects, ~ 10 Gyr, even extremely small values of the rate of change of G can have detectable effects. The first attempts to obtain constraints on $\dot{G}$ from the cooling of white dwarfs (Vila, 1976) were unsuccessful due to the lack of reliable observational data and the uncertainties in the cooling theory of white dwarfs. Since then both the observational data and the cooling theory have been improved substantially, as discussed in Sect. 4. It has been shown (Garcia-Berro et al., 1995) that for the case of a secularly varying G, the luminosity of a cool enough white dwarf is given by:

$$L = -\frac{dB}{dt} + \frac{\dot{G}}{G}\Omega \qquad (12)$$

where $B = U + \Omega$ is the binding energy, U is the thermal energy and Ω is the gravitational energy. As the white dwarf cools, the thermal content decreases and the second term in Eq. (12) dominates. Note as well that the cooling process is accelerated if $\dot{G}/G < 0$. By comparing the results of the previous equation with the observed position of the down-turn in the white dwarf luminosity function, the following firm limit was obtained:

$$-(1 \pm 1) \times 10^{-11} \text{ yr}^{-1} < \frac{\dot{G}}{G} < 0 \qquad (13)$$

at the 1σ confidence level (Garcia-Berro et al., 1995). This result was challenged by Benvenuto et al. (1999), who obtained a much tighter bound using the same method, but their analysis was subsequently shown to be flawed. This issue was finally settled by detailed evolutionary calculations (Althaus et al., 2011; García-Berro et al., 2011a), which corroborated the preliminary analytical calculations of Garcia-Berro et al. (1995). We mention here that a tighter bound was obtained by García-Berro et al. (2011b) using the white dwarf luminosity function of the open, metal-rich, well-populated cluster NGC 6791:

$$-1.8 \times 10^{-12} \text{ yr}^{-1} < \frac{\dot{G}}{G} < 0 \qquad (14)$$

The last and most exotic application of the white dwarf luminosity function we would like to discuss here is its use as an astro-particle physics laboratory. Pulsating white dwarfs have been used frequently for such a purpose (Fontaine et al., 2001). For example, the plasma neutrino process has been tested using pulsating DB white dwarfs — see Winget et al. (2004), and references therein. The existence of neutrinos has been known for many years, yet there are other exotic particles that have been postulated by theorists that have not been detected so far. The white dwarf luminosity function can help in this regard. For instance, the mass of the axion has been constrained using ZZ Ceti white dwarfs (Córsico et al., 2001; Isern et al., 2010; Miller Bertolami et al., 2014). The white dwarf luminosity function appears to leave little room for other theorized weakly interacting exotic particles such as "massive dark photons and "dark sector particles" lighter than a few keV (Dreiner et al., 2013; Ubaldi, 2014). It has also been shown very recently that the white dwarf luminosity function can be used to derive consistent upper limits to the mass of the axion, and the axion-electron coupling constant (g_{ae}) of DFSZ-axions (Isern et al., 2008). Clearly, more accurate constraints would be enabled by improved observational white dwarf luminosity functions.

7. The future

Although it has been used to construct nearly every white dwarf luminosity function to date, the $1/\mathcal{V}_{max}$ technique is very vulnerable to undetected incompleteness and small sample statistical uncertainties. It has been shown — see, for instance, Sect. 3.1, Wood and Oswalt (1998), and García-Berro et al. (1999) — that the age estimate resulting from the $1/\mathcal{V}_{max}$ method is also very sensitive to the choice of assumed Galactic disk scale height, binning interval, placement of bin centers, and that the space density is inherently uncertain by at least 50% in samples containing less than ~ 100 stars. Also, the vast majority of known white dwarfs do not meet the completeness magnitude and proper motion limits imposed by the $1/\mathcal{V}_{max}$ technique, so they cannot be included in the standard white dwarf luminosity function. It has been shown (Geijo et al., 2006) that other techniques not previously used on white dwarfs do better in identifying the luminosity down-turn and the total space density. It will be important to use more sophisticated techniques such as these on the large samples of white dwarfs that will be available soon.

The next decade holds much promise for a definitive determination of the

white dwarf luminosity function for each of the three major stellar components of the solar neighborhood. Among the first opportunities for improvement will be PanSTARRS data (Kaiser et al., 2002), which will cover the entire sky observed in the course of the SDSS on timescales of less than a week, reaching 24th magnitude in each frame — 2–3 magnitudes fainter than the best large area surveys available today. PanSTARRS opens a new time domain on the sky that has exciting potential for discovery in a wide range of astronomy, ranging from the search for near earth asteroids to gamma ray burster afterglows. Two of the science objectives of PanSTARRS will contribute directly to improving the white dwarf luminosity function. The Solar Neighborhood (SOL) project will build an all-sky parallax catalog for stars within ~ 100 pc over its ten-year lifetime. It is expected to provide a volume-limited sample out to ~ 50 pc suitable for studies of brown dwarf stars and cool white dwarfs. The Extragalactic and Galactic Stellar Science (EGGS) project will provide a proper motion catalog for $\sim 10^8$ stars, whose precision reaches $\sim 1\,\mathrm{mas/yr}$. This astrometric database will be a goldmine for white dwarf searches, especially in the halo, via reduced proper motion diagrams. The astrometric grid established by PanSTARRS also will comprise a faint object reference catalog for higher precision but sparser surveys such as Gaia.

In a sense, PanSTARRS is a pilot project for the Large-aperture Synoptic Survey Telescope (LSST) project. The LSST is a proposed ground-based 8.4-meter, 10 square-degree-field telescope that will image the entire sky every three nights in continuous 30-second exposures. It will open a movie-like window on the sky. One of the proposed by-products of the data stream is a parallax catalog. Assuming astrometric precision of a few μas per observation, it has been shown (Ivezic et al., 2008; Covey et al., 2010) that short-arc parallaxes can be measured for stars out to 10 pc in a few months of observation. LSST multi-band photometry will permit the determination of photometric parallaxes, chemical abundances and ages via colors at the turn-off for main-sequence stars at all distances within the Galaxy. With a geometric parallax accuracy of 1 milli-arcsecond and exposures reaching $g = 25$, the LSST parallax survey will match the faint-end precision of planned space-based missions like Gaia, providing a complete catalog to at least $M_\mathrm{v} = 15$ through the half of the Galaxy visible from its site in Chile.

One of the most-anticipated astrometric surveys will be conducted by the ESA satellite Gaia (Perryman et al., 2001). It is expected to yield high precision parallaxes as well as proper motions. The typical accuracy of the

parallaxes will be of the order of 26 μas at $V = 15$, degrading to 600 μas at $V = 20$. The measured proper motions will be good to 0.2 mas per year. Gaia will provide multi-color photometry for 1.3 billion stars at $V = 20$. Also, it was expected to measure radial velocities to a few km/s precision to at least $V = 17$ (Jordan and de Bruijne, 2013), but recently discovered scattered light problems will probably reduce the performance of radial velocity spectrometer to $V = 15$. In any case, Gaia's spectroscopic instrument is specifically designed to work around the near-infrared Ca triplet and so will be useless for most white dwarfs. Nevertheless, Gaia will generate an unprecedented sample of stars from which to construct the white dwarf luminosity function for all three components of the Galaxy. Specifically, it is foreseen that Gaia will discover around 400,000 new white dwarfs (Jordan, 2007). Using a population synthesis code Torres et al. (2005) showed that the disk white dwarf population can be probed out to at least 400 pc and apparent Gaia magnitude $G = 21$. Distinguishing between disk and halo white dwarfs will require fairly sophisticated automatic classification algorithms (Torres et al., 1998) in addition to the usual reduced proper motion diagrams. The age of the disk and space density of disk white dwarfs will be well-determined, and hypothetical merger episodes in the disk can be investigated. However, due to the poor sensitivity of Gaia's detectors at red wavelengths, most likely only the bright half of the halo white dwarf luminosity function will be probed (Torres et al., 2005).

8. Summary of age and space density determinations

Here we summarize the most relevant observational estimates of the ages and space densities of white dwarfs discussed in Sects. 2 and 7. We do not pretend to be exhaustive, but provide an overview of the results obtained from what we consider to be the most relevant observational data sets. Table 2 shows the local white dwarf space densities for the Galactic disk (top sections) and halo (bottom section). Also shown in this table are the derived age, when available (first column), the number of stars in the sample (second column), the source (third column) and the appropriate reference (last column). As can be seen, the estimated space densities of disk white dwarfs are fairly consistent — except for the very initial studies. A simple average yields 4.3×10^{-3} pc^{-3}. This estimate is uncertain by at least 10%. The estimates of the white dwarf number density for the halo population are rather discrepant, but the most recent estimates indicate that the white

Table 2: Summary of the space densities of disk — top sections, in units of 10^{-3} pc^{-3} — and halo white dwarfs — bottom section, in units of 10^{-6} pc^{-3} — obtained by different authors.

Age (Gyr)	Sample size	Source	n	References
		Disk (All white dwarfs)		
—	23	10 pc sample	> 5	Sion and Liebert (1977)
—	20	Proper motion	7.5	Eggen (1983)
9.3 ± 2.0	43	Field white dwarfs	3.0	Winget et al. (1987); Liebert et al. (1988)
$9.5^{+1.1}_{-0.8}$	50	Wide binaries	$5.3^{+3.5}_{-0.7}$	Oswalt et al. (1996)
8.0 ± 1.5	43	Liebert et al. (1988)	3.39	Leggett et al. (1998)
10.0^{+3}_{-1}	53	Proper motion	4.16	Knox et al. (1999)
—	43	Liebert et al. (1988); Leggett et al. (1998)	2.5	Méndez and Ruiz (2001)
7.5	46	13 pc sample	5.0 ± 0.7	Holberg et al. (2002); Cignoni et al. (2003)
—	$\sim 6,000$	SDSS	4.6 ± 0.5	Harris et al. (2006)
—	44	13 pc sample	4.8 ± 0.5	Holberg et al. (2008)
—	3,358	SDSS	—	De Gennaro et al. (2008)
—	8	Deep field	$3.46^{+1.71}_{-1.20}$	Silvotti et al. (2009)
—	$\sim 10^4$	Proper motion	3.19 ± 0.09	Rowell and Hambly (2011)
		Disk (Hot white dwarf samples)		
—	353	Hot PG white dwarfs only	0.49 ± 0.05	Fleming et al. (1986)
—	41	Hot AAT white dwarfs only	0.60 ± 0.09	Boyle (1989)
—	298	Hot PG white dwarfs only	0.50 ± 0.05	Liebert et al. (2005)
		Halo		
—	6	Proper motion	13 ± 6	Liebert et al. (1989b)
—	2	Proper motion	~ 700	Ibata et al. (2000)
—	38	Proper motion	~ 220	Oppenheimer et al. (2001)
—	33	SDSS	0.4	Harris et al. (2006)
11.47	~ 1000	Globular clusters	—	Hansen et al. (2007)
—	$\sim 10^4$	Proper motion	4.4 ± 1.3	Rowell and Hambly (2011)
10–11	3	SDSS	—	Kilic et al. (2010)

dwarf number density in the halo is two to three orders of magnitude lower than the disk.

Finally, we would like to mention that the white dwarf luminosity function also has provided useful independent age determinations for several globular and open clusters (von Hippel et al., 1995; Claver, 1995; Richer et al., 1998; von Hippel, 1998; von Hippel and Gilmore, 2000). These and other investigations of the white dwarf luminosity function in clusters will not be discussed in detail here. Let us mention, however, that clusters provide useful benchmarks for the relative ages of the disk and halo, but they do not span the entire age range of their parent populations. Each of these components is also subject to different influences that can bias the derived luminosity functions. In the halo, globular clusters are subject to uncertainties in distance determinations, limiting magnitudes, abundances, mass segregation, tidal stripping, binary interactions, and/or deficiencies in evolutionary models (von Hippel, 1998; Richer et al., 2000; Hurley and Shara, 2003; Hansen et al., 2004). In the disk, the white dwarf luminosity functions of open clusters sometimes provide ages (Bedin et al., 2005) that sharply contrast with those derived from main-sequence turn-off ages, if all the energy sources are not properly taken into account (García-Berro et al., 2010, 2011c). Clearly there is much left to be done in this area.

9. Conclusions

The field has advanced in several distinct ways since the first robust white dwarf luminosity function was constructed (Liebert et al., 1988). Substantial samples of white dwarfs from the thin and thick disk have been assembled. Convincing samples of halo white dwarfs have been identified, though they still are too small to allow construction of a definitive luminosity function. The white dwarf luminosity functions for open clusters and globular clusters are beginning to provide useful time markers for the early history of the Galaxy.

Probably the most significant improvements during the last decade have been in the theoretical models for white dwarfs, which now incorporate more realistic core cooling physics and atmospheric opacities. In addition, artificial samples of white dwarfs have been constructed that have helped quantify the uncertainties in age and space density derived from the white dwarf luminosity function, and how the precision of these important quantities

are related to various binning strategies, sample sizes, population groups, selection biases, among other effects.

Certainly, the next decade will see a dramatic increase in the number of known white dwarfs. More than anything else, this will preserve the status of the white dwarf luminosity function as one of the most important tools for unraveling the origin and evolution of the Galaxy.

Acknowledgments

References

Abrikosov, A., Apr. 1961. Some properties of strongly compressed matter. Sov. Phys. JETP 12, 1254.

Adams, F. C., Laughlin, G., Sep. 1996. Implications of White Dwarf Galactic Halos. ApJ 468, 586.

Alam, S., Albareti, F. D., Allende Prieto, C., Anders, F., Anderson, S. F., Anderton, T., Andrews, B. H., Armengaud, E., Aubourg, É., Bailey, S., et al., Jul. 2015. The Eleventh and Twelfth Data Releases of the Sloan Digital Sky Survey: Final Data from SDSS-III. ApJS 219, 12.

Alcock, C., Allsman, R. A., Alves, D., Axelrod, T. S., Becker, A. C., Bennett, D. P., Cook, K. H., Freeman, K. C., Griest, K., Guern, J., Lehner, M. J., Marshall, S. L., Peterson, B. A., Pratt, M. R., Quinn, P. J., Rodgers, A. W., Stubbs, C. W., Sutherland, W., Welch, D. L., Sep. 1997. The MACHO Project Large Magellanic Cloud Microlensing Results from the First Two Years and the Nature of the Galactic Dark Halo. ApJ 486, 697–726.

Alcock, C., Allsman, R. A., Alves, D., Axelrod, T. S., Bennett, D. P., Cook, K. H., Freeman, K. C., Griest, K., Guern, J., Lehner, M. J., Marshall, S. L.,

Peterson, B. A., Pratt, M. R., Quinn, P. J., Rodgers, A. W., Stubbs, C. W., Sutherland, W., Dec. 1995. First Observation of Parallax in a Gravitational Microlensing Event. ApJ 454, L125.

Alcock, C., Allsman, R. A., Alves, D. R., Axelrod, T. S., Becker, A. C., Bennett, D. P., Cook, K. H., Dalal, N., Drake, A. J., Freeman, K. C., Geha, M., Griest, K., Lehner, M. J., Marshall, S. L., Minniti, D., Nelson, C. A., Peterson, B. A., Popowski, P., Pratt, M. R., Quinn, P. J., Stubbs, C. W., Sutherland, W., Tomaney, A. B., Vandehei, T., Welch, D., Oct. 2000. The MACHO Project: Microlensing Results from 5.7 Years of Large Magellanic Cloud Observations. ApJ 542, 281–307.

Allen, C. W., 1973. Astrophysical quantities, 3rd ed. London: University of London, Athlone Press.

Althaus, L. G., Camisassa, M. E., Miller Bertolami, M. M., Córsico, A. H., García-Berro, E., Feb. 2015. White dwarf evolutionary sequences for low-metallicity progenitors: The impact of third dredge-up. A&A , in press.

Althaus, L. G., Córsico, A. H., Isern, J., García-Berro, E., Oct. 2010a. Evolutionary and pulsational properties of white dwarf stars. A&A Rev. 18, 471–566.

Althaus, L. G., Córsico, A. H., Miller Bertolami, M. M., García-Berro, E., Kepler, S. O., Apr. 2008. Evidence of Thin Helium Envelopes in PG 1159 Stars. ApJ 677, L35–L38.

Althaus, L. G., Córsico, A. H., Torres, S., Lorén-Aguilar, P., Isern, J., García-Berro, E., Mar. 2011. The evolution of white dwarfs with a varying gravitational constant. A&A 527, A72.

Althaus, L. G., García-Berro, E., Isern, J., Córsico, A. H., Oct. 2005a. Mass-radius relations for massive white dwarf stars. A&A 441, 689–694.

Althaus, L. G., García-Berro, E., Isern, J., Córsico, A. H., Miller Bertolami, M. M., Jan. 2012. New phase diagrams for dense carbon-oxygen mixtures and white dwarf evolution. A&A 537, A33.

Althaus, L. G., García-Berro, E., Isern, J., Córsico, A. H., Rohrmann, R. D., Apr. 2007. The age and colors of massive white dwarf stars. A&A 465, 249–255.

Althaus, L. G., García-Berro, E., Renedo, I., Isern, J., Córsico, A. H., Rohrmann, R. D., Aug. 2010b. Evolution of White Dwarf Stars with High-metallicity Progenitors: The Role of ^{22}Ne Diffusion. ApJ 719, 612–621.

Althaus, L. G., Serenelli, A. M., Benvenuto, O. G., May 2001a. Diffusion and the occurrence of hydrogen-shell flashes in helium white dwarf stars. MNRAS 323, 471–483.

Althaus, L. G., Serenelli, A. M., Benvenuto, O. G., Jun. 2001b. The impact of element diffusion on the formation and evolution of helium white dwarf stars. MNRAS 324, 617–622.

Althaus, L. G., Serenelli, A. M., Panei, J. A., Córsico, A. H., García-Berro, E., Scóccola, C. G., May 2005b. The formation and evolution of hydrogen-deficient post-AGB white dwarfs: The emerging chemical profile and the expectations for the PG 1159-DB-DQ evolutionary connection. A&A 435, 631–648.

Andrews, J. J., Agüeros, M. A., Gianninas, A., Kilic, M., Dhital, S., Anderson, S. F., Dec. 2015. Constraints on the Initial-Final Mass Relation from Wide Double White Dwarfs. ApJ 815, 63.

Barrat, J. L., Hansen, J. P., Mochkovitch, R., Jun. 1988. Crystallization of carbon-oxygen mixtures in white dwarfs. A&A 199, L15–L18.

Becker, A. C., Rest, A., Stubbs, C., Miknaitis, G. A., Miceli, A., Covarrubias, R., Hawley, S. L., Aguilera, C., Smith, R. C., Suntzeff, N. B., Olsen, K., Prieto, J. L., Hiriart, R., Garg, A., Welch, D. L., Cook, K. H., Nikolaev, S., Clocchiatti, A., Minniti, D., Keller, S. C., Schmidt, B. P., Jun. 2005. The SuperMACHO Microlensing Survey. In: Mellier, Y., Meylan, G. (Eds.), Gravitational Lensing Impact on Cosmology. Vol. 225 of IAU Symposium. pp. 357–362.

Bedin, L. R., Salaris, M., Piotto, G., King, I. R., Anderson, J., Cassisi, S., Momany, Y., May 2005. The White Dwarf Cooling Sequence in NGC 6791. ApJ 624, L45–L48.

Benvenuto, O. G., Althaus, L. G., Jan. 1998. Evolution of helium white dwarfs with hydrogen envelopes. MNRAS 293, 177.

Benvenuto, O. G., Althaus, L. G., Feb. 1999. Grids of white dwarf evolutionary models with masses from M=0.1 to 1.2 m_solar. MNRAS 303, 30–38.

Benvenuto, O. G., Althaus, L. G., Torres, D. F., May 1999. Evolution of white dwarfs as a probe of theories of gravitation: the case of Brans-Dicke. MNRAS 305, 905–919.

Bergeron, P., Leggett, S. K., Ruiz, M. T., Apr. 2001. Photometric and Spectroscopic Analysis of Cool White Dwarfs with Trigonometric Parallax Measurements. ApJS 133, 413–449.

Bergeron, P., Ruiz, M. T., Leggett, S. K., Jan. 1997. The Chemical Evolution of Cool White Dwarfs and the Age of the Local Galactic Disk. ApJS 108, 339–387.

Bergeron, P., Saffer, R. A., Liebert, J., Jul. 1992. A spectroscopic determination of the mass distribution of DA white dwarfs. ApJ 394, 228–247.

Bergeron, P., Saumon, D., Wesemael, F., Apr. 1995. New model atmospheres for very cool white dwarfs with mixed H/He and pure He compositions. ApJ 443, 764–779.

Bildsten, L., Hall, D. M., Mar. 2001. Gravitational Settling of ^{22}NE in Liquid White Dwarf Interiors. ApJ 549, L219–L223.

Binney, J., Merrifield, M., 1998. Galactic astronomy. Princeton University Press (Princeton, NJ).

Boyle, B. J., Oct. 1989. The space distribution of DA white dwarfs. MNRAS 240, 533–549.

Bravo, E., Isern, J., Canal, R., Labay, J., Apr. 1992. On the contribution of Ne-22 to the synthesis of Fe-54 and Ni-58 in thermonuclear supernovae. A&A 257, 534–538.

Brocato, E., Castellani, V., Romaniello, M., May 1999. A theoretical exploratory investigation on cluster white dwarfs. A&A 345, 499–504.

Butkevich, A. G., Berdyugin, A. V., Teerikorpi, P., Sep. 2005. Statistical biases in stellar astronomy: the Malmquist bias revisited. MNRAS 362, 321–330.

Camacho, J., Torres, S., Isern, J., Althaus, L. G., García-Berro, E., Aug. 2007. The contribution of oxygen-neon white dwarfs to the MACHO content of the Galactic halo. A&A 471, 151–158.

Carrasco, J. M., Catalán, S., Jordi, C., Tremblay, P.-E., Napiwotzki, R., Luri, X., Robin, A. C., Kowalski, P. M., May 2014. Gaia photometry for white dwarfs. A&A 565, A11.

Casewell, S. L., Dobbie, P. D., Napiwotzki, R., Burleigh, M. R., Barstow, M. A., Jameson, R. F., Jun. 2009. High-resolution optical spectroscopy of Praesepe white dwarfs. MNRAS 395, 1795–1804.

Catalán, S., Isern, J., García-Berro, E., Ribas, I., Jul. 2008a. The initial-final mass relationship of white dwarfs revisited: effect on the luminosity function and mass distribution. MNRAS 387, 1693–1706.

Catalán, S., Isern, J., García-Berro, E., Ribas, I., Allende Prieto, C., Bonanos, A. Z., Jan. 2008b. The initial-final mass relationship from white dwarfs in common proper motion pairs. A&A 477, 213–221.

Chabrier, G., Brassard, P., Fontaine, G., Saumon, D., Nov. 2000. Cooling Sequences and Color-Magnitude Diagrams for Cool White Dwarfs with Hydrogen Atmospheres. ApJ 543, 216–226.

Chen, E. Y., Hansen, B. M. S., Jul. 2012. The Spectral Evolution of Convective Mixing White Dwarfs, the Non-DA Gap, and White Dwarf Cosmochronology. ApJ 753, L16.

Choloniewski, J., Nov. 1986. New method for the determination of the luminosity function of galaxies. MNRAS 223, 1–9.

Cignoni, M., Degl'Innocenti, S., Castellani, V., Prada Moroni, P. G., Petroni, S., 2003. The Galactic white dwarf populations. Mem. Soc. Astron. Ital. 74, 454.

Claver, C., May 1995. The age of the Milky Way galaxy from white dwarf chronometry. Ph.D. thesis, University of Texas at Austin.

Cojocaru, R., Torres, S., Isern, J., García-Berro, E., Jun. 2014. The effects of metallicity on the Galactic disk population of white dwarfs. A&A 566, A81.

Córsico, A. H., Benvenuto, O. G., Althaus, L. G., Isern, J., García-Berro, E., Jun. 2001. The potential of the variable DA white dwarf G117-B15A as a tool for fundamental physics. New Astron. 6, 197–213.

Covey, K. R., Saha, A., Beers, T. C., Bochanski, J. J., Boeshaar, P., Burgasser, A., Cargile, P., Chu, Y., Claver, C., Cook, K., Dhital, S., Hawley, S. L., Hebb, L., Henry, T. J., Hilton, E., Holberg, J. B., Ivezic, Z., Juric, M. L., Kafka, S., Kalirai, J., Lepine, S., Macri, L., McGehee, P. M., Monet, D., Olsen, K., Pepper, J., Prsa, A., Sarajedini, A., Silvestri, N., Stassun, K., Thorman, P., West, A. A., Williams, B. F., Jan. 2010. Stellar Population Science with LSST. In: American Astronomical Society Meeting Abstracts #215. Vol. 42 of Bulletin of the American Astronomical Society. p. 401.08.

D'Antona, F., Mazzitelli, I., Dec. 1989. The fastest evolving white dwarfs. ApJ 347, 934–949.

Darling, G. W., Jan. 1994. Cosmology from the KISO Ultraviolet Excess Survey: a Complete Sample of White Dwarfs and Quasars. Ph.D. thesis, DARTMOUTH COLLEGE.

De Gennaro, S., von Hippel, T., Winget, D. E., Kepler, S. O., Nitta, A., Koester, D., Althaus, L., Jan. 2008. White Dwarf Luminosity and Mass Functions from Sloan Digital Sky Survey Spectra. AJ 135, 1–9.

Deloye, C. J., Bildsten, L., Dec. 2002. Gravitational Settling of ^{22}Ne in Liquid White Dwarf Interiors: Cooling and Seismological Effects. ApJ 580, 1077–1090.

Diaz-Pinto, A., Garcia-Berro, E., Hernanz, M., Isern, J., Mochkovitch, R., Feb. 1994. The luminosity function of massive white dwarfs. A&A 282, 86–92.

Dobbie, P. D., Napiwotzki, R., Burleigh, M. R., Barstow, M. A., Boyce, D. D., Casewell, S. L., Jameson, R. F., Hubeny, I., Fontaine, G., Jun. 2006. New Praesepe white dwarfs and the initial mass-final mass relation. MNRAS 369, 383–389.

Dobbie, P. D., Napiwotzki, R., Burleigh, M. R., Williams, K. A., Sharp, R., Barstow, M. A., Casewell, S. L., Hubeny, I., Jun. 2009. A new detailed

examination of white dwarfs in NGC 3532 and NGC 2287. MNRAS 395, 2248–2256.

Domínguez, I., Chieffi, A., Limongi, M., Straniero, O., Oct. 1999. Intermediate-Mass Stars: Updated Models. ApJ 524, 226–241.

Dreiner, H. K., Fortin, J.-F., Isern, J., Ubaldi, L., Aug. 2013. White dwarfs constrain dark forces. Phys. Rev. D 88 (4), 043517.

Driebe, T., Blöcker, T., Schönberner, D., Herwig, F., Oct. 1999. The evolution of helium white dwarfs. II. Thermal instabilities. A&A 350, 89–100.

Driebe, T., Schoenberner, D., Bloecker, T., Herwig, F., Nov. 1998. The evolution of helium white dwarfs. I. The companion of the millisecond pulsar PSR J1012+5307. A&A 339, 123–133.

Efstathiou, G., Ellis, R. S., Peterson, B. A., May 1988. Analysis of a complete galaxy redshift survey. II - The field-galaxy luminosity function. MNRAS 232, 431–461.

Eggen, O. J., Feb. 1983. Luminosity and motion of large proper motion stars. II - Stars with annual proper motion larger than 0.7 arc seconds. ApJS 51, 183–202.

Eggen, O. J., Greenstein, J. L., Jan. 1965. Spectra, colors, luminosities, and motions of the white dwarfs. ApJ 141, 83.

Farihi, J., Aug. 2004. Discovery of an Ultracool White Dwarf Companion. ApJ 610, 1013–1020.

Farihi, J., Becklin, E. E., Zuckerman, B., Dec. 2005. Low-Luminosity Companions to White Dwarfs. ApJS 161, 394–428.

Felten, J. E., Aug. 1976. On Schmidt's Vm estimator and other estimators of luminosity functions. ApJ 207, 700–709.

Ferrario, L., Wickramasinghe, D., Liebert, J., Williams, K. A., Aug. 2005. The open-cluster initial-final mass relationship and the high-mass tail of the white dwarf distribution. MNRAS 361, 1131–1135.

Finley, D. S., Koester, D., Nov. 1997. PG 0922+162: Discovery of the Youngest Visual Double Degenerate. ApJ 489, L79–L82.

Fleming, T. A., Liebert, J., Green, R. F., Sep. 1986. The luminosity function of DA white dwarfs. ApJ 308, 176–189.

Flynn, C., Sommer-Larsen, J., Fuchs, B., Graff, D. S., Salim, S., Apr. 2001. A search for nearby counterparts to the moving objects in the Hubble Deep Field. MNRAS 322, 553–560.

Fontaine, G., Bergeron, P., Brassard, P., 2005. Old ultracool white dwarfs as cosmological probes. In: Sion, E. M., Vennes, S., Shipman, H. L. (Eds.), White dwarfs: cosmological and galactic probes. Vol. 332 of Astrophysics and Space Science Library. pp. 3–13.

Fontaine, G., Brassard, P., Bergeron, P., Apr. 2001. The Potential of White Dwarf Cosmochronology. PASP 113, 409–435.

Garcia-Berro, E., Hernanz, M., Isern, J., Chabrier, G., Segretain, L., Mochkovitch, R., May 1996. A simple method to compute white dwarf luminosity functions. A&AS 117, 13–18.

Garcia-Berro, E., Hernanz, M., Isern, J., Mochkovitch, R., Jun. 1988. Properties of high-density binary mixtures and the age of the universe from white dwarf stars. Nature 333, 642–644.

Garcia-Berro, E., Hernanz, M., Isern, J., Mochkovitch, R., Dec. 1995. The rate of change of the gravitational constant and the cooling of white dwarfs. MNRAS 277, 801–810.

Garcia-Berro, E., Iben, I., Oct. 1994. On the formation and evolution of super-asymptotic giant branch stars with cores processed by carbon burning. 1: SPICA to Antares. ApJ 434, 306–318.

Garcia-Berro, E., Isern, J., Hernanz, M., Aug. 1997. The cooling of oxygen-neon white dwarfs. MNRAS 289, 973–978.

García-Berro, E., Lorén-Aguilar, P., Torres, S., Althaus, L. G., Isern, J., May 2011a. An upper limit to the secular variation of the gravitational constant from white dwarf stars. J. Cosmol. & Astropart. Phys. 5, 21.

García-Berro, E., Lorén-Aguilar, P., Torres, S., Althaus, L. G., Isern, J., May 2011b. An upper limit to the secular variation of the gravitational constant from white dwarf stars. J. Cosmol. & Astropart. Phys. 5, 21.

García-Berro, E., Torres, S., Althaus, L. G., Renedo, I., Lorén-Aguilar, P., Córsico, A. H., Rohrmann, R. D., Salaris, M., Isern, J., May 2010. A white dwarf cooling age of 8Gyr for NGC 6791 from physical separation processes. Nature 465, 194–196.

García-Berro, E., Torres, S., Isern, J., Burkert, A., Jan. 1999. Monte Carlo simulations of the disc white dwarf population. MNRAS 302, 173–188.

García-Berro, E., Torres, S., Isern, J., Burkert, A., Apr. 2004. Monte Carlo simulations of the halo white dwarf population. A&A 418, 53–65.

García-Berro, E., Torres, S., Renedo, I., Camacho, J., Althaus, L. G., Córsico, A. H., Salaris, M., Isern, J., Sep. 2011c. The white-dwarf cooling sequence of NGC 6791: a unique tool for stellar evolution. A&A 533, A31.

Geijo, E. M., Torres, S., Isern, J., García-Berro, E., Jul. 2006. The white dwarf luminosity function - I. Statistical errors and alternatives. MNRAS 369, 1654–1666.

Gentile Fusillo, N. P., Rebassa-Mansergas, A., Gänsicke, B. T., Liu, X.-W., Ren, J. J., Koester, D., Zhan, Y., Hou, Y., Wang, Y., Yang, M., Sep. 2015. An independent test of the photometric selection of white dwarf candidates using LAMOST DR3. MNRAS 452, 765–773.

Giammichele, N., Bergeron, P., Dufour, P., Apr. 2012. Know Your Neighborhood: A Detailed Model Atmosphere Analysis of Nearby White Dwarfs. ApJS 199, 29.

Gibson, B. K., Mould, J. R., Jun. 1997. The Chemical Residue of a White Dwarf-dominated Galactic Halo. ApJ 482, 98–103.

Girardi, L., Bressan, A., Bertelli, G., Chiosi, C., Feb. 2000. Evolutionary tracks and isochrones for low- and intermediate-mass stars: From 0.15 to 7 M$_{sun}$, and from Z=0.0004 to 0.03. A&AS 141, 371–383.

Goldman, B., Afonso, C., Alard, C., Albert, J.-N., Amadon, A., Andersen, J., Ansari, R., Aubourg, É., Bareyre, P., Bauer, F., Beaulieu, J.-P., Blanc, G., Bouquet, A., Char, S., Charlot, X., Couchot, F., Coutures, C., Derue, F., Ferlet, R., Fouqué, P., Glicenstein, J.-F., Gould, A., Graff, D., Gros, M., Haissinski, J., Hamadache, C., Hamilton, J.-C., Hardin, D., de Kat, J., Kim, A., Lasserre, T., Le Guillou, L., Lesquoy, É., Loup, C., Magneville,

C., Mansoux, B., Marquette, J.-B., Maurice, É., Maury, A., Milsztajn, A., Moniez, M., Palanque-Delabrouille, N., Perdereau, O., Prévot, L., Regnault, N., Rich, J., Spiro, M., Tisserand, P., Vidal-Madjar, A., Vigroux, L., Zylberajch, S., EROS Collaboration, Jul. 2002. EROS 2 proper motion survey: Constraints on the halo white dwarfs. A&A 389, L69–L73.

Greenstein, J. L., Oct. 1986a. White Dwarfs in Wide Binaries - Part Two - Double Degenerates and Composite Spectra. AJ 92, 867.

Greenstein, J. L., Oct. 1986b. White dwarfs in wide binaries. I - Physical properties. II - Double degenerates and composite spectra. AJ 92, 859–877.

Hambly, N. C., Henry, T. J., Subasavage, J. P., Brown, M. A., Jao, W.-C., Jul. 2004. The Solar Neighborhood. VIII. Discovery of New High Proper Motion Nearby Stars Using the SuperCOSMOS Sky Survey. AJ 128, 437–447.

Hansen, B. M. S., Aug. 1998. Old and blue white-dwarf stars as a detectable source of microlensing events. Nature 394, 860–862.

Hansen, B. M. S., Aug. 1999. Cooling Models for Old White Dwarfs. ApJ 520, 680–695.

Hansen, B. M. S., Anderson, J., Brewer, J., Dotter, A., Fahlman, G. G., Hurley, J., Kalirai, J., King, I., Reitzel, D., Richer, H. B., Rich, R. M., Shara, M. M., Stetson, P. B., Dec. 2007. The White Dwarf Cooling Sequence of NGC 6397. ApJ 671, 380–401.

Hansen, B. M. S., Liebert, J., 2003. Cool White Dwarfs. ARA&A 41, 465–515.

Hansen, B. M. S., Phinney, E. S., Mar. 1998. Stellar forensics. I - Cooling curves. MNRAS 294, 557.

Hansen, B. M. S., Richer, H. B., Fahlman, G. G., Stetson, P. B., Brewer, J., Currie, T., Gibson, B. K., Ibata, R., Rich, R. M., Shara, M. M., Dec. 2004. Hubble Space Telescope Observations of the White Dwarf Cooling Sequence of M4. ApJS 155, 551–576.

Harris, H. C., Dahn, C. C., Vrba, F. J., Henden, A. A., Liebert, J., Schmidt, G. D., Reid, I. N., Oct. 1999. A Very Low Luminosity, Very Cool, DC White Dwarf. ApJ 524, 1000–1007.

Harris, H. C., Munn, J. A., Kilic, M., Liebert, J., Williams, K. A., von Hippel, T., Levine, S. E., Monet, D. G., Eisenstein, D. J., Kleinman, S. J., Metcalfe, T. S., Nitta, A., Winget, D. E., Brinkmann, J., Fukugita, M., Knapp, G. R., Lupton, R. H., Smith, J. A., Schneider, D. P., Jan. 2006. The White Dwarf Luminosity Function from Sloan Digital Sky Survey Imaging Data. AJ 131, 571–581.

Hernanz, M., Garcia-Berro, E., Isern, J., Mochkovitch, R., Segretain, L., Chabrier, G., Oct. 1994. The influence of crystallization on the luminosity function of white dwarfs. ApJ 434, 652–661.

Hintzen, P., Aug. 1986. Spectroscopic observations of cool degenerate star candidates. AJ 92, 431–435.

Holberg, J., Oswalt, T., Sion, E., 2016. The 25 Parsec Local White Dwarf Population. MNRAS , submitted.

Holberg, J. B., Oswalt, T. D., Sion, E. M., May 2002. A Determination of the Local Density of White Dwarf Stars. ApJ 571, 512–518.

Holberg, J. B., Sion, E. M., Oswalt, T., McCook, G. P., Foran, S., Subasavage, J. P., Apr. 2008. A New Look at the Local White Dwarf Population. AJ 135, 1225–1238.

Hollik, W., Nov. 1997. Precision tests of the electroweak theory. Journal of Physics G Nuclear Physics 23, 1503–1537.

Horowitz, C. J., Schneider, A. S., Berry, D. K., Jun. 2010. Crystallization of Carbon-Oxygen Mixtures in White Dwarf Stars. Phys. Rev. Lett. 104 (23), 231101.

Hu, Q., Wu, C., Wu, X.-B., May 2007. The mass and luminosity functions and the formation rate of DA white dwarfs in the Sloan Digital Sky Survey. A&A 466, 627–639.

Hurley, J. R., Shara, M. M., May 2003. White Dwarf Sequences in Dense Star Clusters. ApJ 589, 179–198.

Ibata, R., Irwin, M., Bienaymé, O., Scholz, R., Guibert, J., Mar. 2000. Discovery of High Proper-Motion Ancient White Dwarfs: Nearby Massive Compact Halo Objects? ApJ 532, L41–L45.

Ibata, R. A., Richer, H. B., Gilliland, R. L., Scott, D., Oct. 1999. Faint, Moving Objects in the Hubble Deep Field: Components of the Dark Halo? ApJ 524, L95–L97.

Iben, Jr., I., Laughlin, G., Jun. 1989. A study of the white dwarf luminosity function. ApJ 341, 312–326.

Iben, Jr., I., Tutukov, A. V., Jul. 1984. Cooling of low-mass carbon-oxygen dwarfs from the planetary nucleus stage through the crystallization stage. ApJ 282, 615–630.

Ichimaru, S., Iyetomi, H., Ogata, S., Nov. 1988. Freezing transition and phase diagram of dense carbon-oxygen mixtures in white dwarfs. ApJ 334, L17–L20.

Isern, J., Artigas, A., García-Berro, E., Mar. 2013. White dwarf cooling sequences and cosmochronology. In: European Physical Journal Web of Conferences. Vol. 43 of European Physical Journal Web of Conferences. p. 5002.

Isern, J., García-Berro, E., Althaus, L. G., Córsico, A. H., Mar. 2010. Axions and the pulsation periods of variable white dwarfs revisited. A&A 512, A86.

Isern, J., García-Berro, E., Hernanz, M., Mochkovitch, R., Dec. 1998a. The physics of white dwarfs. Journal of Physics Condensed Matter 10, 11263–11272.

Isern, J., García-Berro, E., Hernanz, M., Mochkovitch, R., Burkert, A., 1995. The Stellar Formation Rate and the White Dwarf Luminosity Function. In: Koester, D., Werner, K. (Eds.), White Dwarfs. Vol. 443 of Lecture Notes in Physics, Berlin Springer Verlag. p. 19.

Isern, J., García-Berro, E., Hernanz, M., Mochkovitch, R., Torres, S., Aug. 1998b. The Halo White Dwarf Population. ApJ 503, 239–246.

Isern, J., García-Berro, E., Salaris, M., 2001. What Are White Dwarfs Telling Us About the Galactic Disk and Halo? In: von Hippel, T., Simpson,

C., Manset, N. (Eds.), Astrophysical Ages and Times Scales. Vol. 245 of Astronomical Society of the Pacific Conference Series. p. 328.

Isern, J., García-Berro, E., Torres, S., Catalán, S., Aug. 2008. Axions and the Cooling of White Dwarf Stars. ApJ 682, L109–L112.

Isern, J., Hernanz, M., Mochkovitch, R., Garcia-Berro, E., Jan. 1991. The role of the minor chemical species in the cooling of white dwarfs. A&A 241, L29–L32.

Isern, J., Mochkovitch, R., García-Berro, E., Hernanz, M., Aug. 1997. The Physics of Crystallizing White Dwarfs. ApJ 485, 308–312.

Ivezic, Z., Axelrod, T., Brandt, W. N., Burke, D. L., Claver, C. F., Connolly, A., Cook, K. H., Gee, P., Gilmore, D. K., Jacoby, S. H., Jones, R. L., Kahn, S. M., Kantor, J. P., Krabbendam, V. V., Lupton, R. H., Monet, D. G., Pinto, P. A., Saha, A., Schalk, T. L., Schneider, D. P., Strauss, M. A., Stubbs, C. W., Sweeney, D., Szalay, A., Thaler, J. J., Tyson, J. A., LSST Collaboration, Jun. 2008. Large Synoptic Survey Telescope: From Science Drivers To Reference Design. Serbian Astronomical Journal 176, 1–13.

Jones, E. M., Nov. 1972. Reduced-Proper Diagrams. II. Luyten's White-Dwarf Catalog. ApJ 177, 245.

Jordan, S., Sep. 2007. Gaia — A White Dwarf Discovery Machine. In: Napiwotzki, R., Burleigh, M. R. (Eds.), 15th European Workshop on White Dwarfs. Vol. 372 of Astronomical Society of the Pacific Conference Series. p. 139.

Jordan, S., de Bruijne, J., Jan. 2013. Astrometric Determination of White Dwarf Radial Velocities with Gaia? In: Krzesiń, ski, J., Stachowski, G., Moskalik, P., Bajan, K. (Eds.), 18th European White Dwarf Workshop. Vol. 469 of Astronomical Society of the Pacific Conference Series. p. 257.

Kaiser, N., Aussel, H., Burke, B. E., Boesgaard, H., Chambers, K., Chun, M. R., Heasley, J. N., Hodapp, K.-W., Hunt, B., Jedicke, R., Jewitt, D., Kudritzki, R., Luppino, G. A., Maberry, M., Magnier, E., Monet, D. G., Onaka, P. M., Pickles, A. J., Rhoads, P. H. H., Simon, T., Szalay, A., Szapudi, I., Tholen, D. J., Tonry, J. L., Waterson, M., Wick, J., Dec. 2002. Pan-STARRS: A Large Synoptic Survey Telescope Array. In: Tyson, J. A.,

Wolff, S. (Eds.), Survey and Other Telescope Technologies and Discoveries. Vol. 4836 of Society of Photo-Optical Instrumentation Engineers (SPIE) Conference Series. pp. 154–164.

Kalirai, J. S., Hansen, B. M. S., Kelson, D. D., Reitzel, D. B., Rich, R. M., Richer, H. B., Mar. 2008. The Initial-Final Mass Relation: Direct Constraints at the Low-Mass End. ApJ 676, 594–609.

Karakas, A. I., Lattanzio, J. C., Pols, O. R., 2002. Parameterising the Third Dredge-up in Asymptotic Giant Branch Stars. Pub. Astr. Soc. Australia 19, 515–526.

Kawka, A., Vennes, S., May 2006. Spectroscopic Identification of Cool White Dwarfs in the Solar Neighborhood. ApJ 643, 402–415.

Kepler, S. O., Pelisoli, I., Koester, D., Ourique, G., Kleinman, S. J., Romero, A. D., Nitta, A., Eisenstein, D. J., Costa, J. E. S., Külebi, B., Jordan, S., Dufour, P., Giommi, P., Rebassa-Mansergas, A., Feb. 2015. New white dwarf stars in the Sloan Digital Sky Survey Data Release 10. MNRAS 446, 4078–4087.

Kilic, M., Mendez, R. A., von Hippel, T., Winget, D. E., Nov. 2005. Faint Blue Objects in the Hubble Deep Field-South Revealed: White Dwarfs, Subdwarfs, and Quasars. ApJ 633, 1126–1141.

Kilic, M., Munn, J. A., Harris, H. C., Liebert, J., von Hippel, T., Williams, K. A., Metcalfe, T. S., Winget, D. E., Levine, S. E., Jan. 2006. Cool White Dwarfs in the Sloan Digital Sky Survey. AJ 131, 582–599.

Kilic, M., Munn, J. A., Williams, K. A., Kowalski, P. M., von Hippel, T., Harris, H. C., Jeffery, E. J., DeGennaro, S., Brown, W. R., McLeod, B., May 2010. Visitors from the Halo: 11 Gyr Old White Dwarfs in the Solar Neighborhood. ApJ 715, L21–L25.

Kirshnitz, D. A., Apr. 1960. On the internal structure of superdense stars. Sov. Phys. JETP 11, 365.

Knox, R. A., Hawkins, M. R. S., Hambly, N. C., Jul. 1999. A survey for cool white dwarfs and the age of the Galactic disc. MNRAS 306, 736–752.

Koester, D., 2002. White dwarfs: Recent developments. A&A Rev. 11, 33–66.

Koester, D., Schoenberner, D., Jan. 1986. Evolution of white dwarfs. A&A 154, 125–134.

Kondo, M., Noguchi, T., Maehara, H., 1984. A search for ultraviolet-excess objects. II. Annals of the Tokyo Astronomical Observatory 20, 130–189.

Kordopatis, G., Binney, J., Gilmore, G., Wyse, R. F. G., Belokurov, V., McMillan, P. J., Hatfield, P., Grebel, E. K., Steinmetz, M., Navarro, J. F., Seabroke, G., Minchev, I., Chiappini, C., Bienaymé, O., Bland-Hawthorn, J., Freeman, K. C., Gibson, B. K., Helmi, A., Munari, U., Parker, Q., Reid, W. A., Siebert, A., Siviero, A., Zwitter, T., Mar. 2015. The rich are different: evidence from the RAVE survey for stellar radial migration. MNRAS 447, 3526–3535.

Kroupa, P., Apr. 2001. On the variation of the initial mass function. MNRAS 322, 231–246.

Kroupa, P., Jan. 2002. The Initial Mass Function of Stars: Evidence for Uniformity in Variable Systems. Science 295, 82–91.

Krzesinski, J., Jan. 2013. Hot White Dwarf Luminosity Function, non-DA to DA Ratio, SDSS DR7: Possible Improvements. In: Krzesiński, J., Stachowski, G., Moskalik, P., Bajan, K. (Eds.), 18th European White Dwarf Workshop. Vol. 469 of Astronomical Society of the Pacific Conference Series. p. 77.

Krzesinski, J., Kleinman, S. J., Nitta, A., Hügelmeyer, S., Dreizler, S., Liebert, J., Harris, H., Dec. 2009. A hot white dwarf luminosity function from the Sloan Digital Sky Survey. A&A 508, 339–344.

Krzesinski, J., Torres, S., García–Berro, E., Jun. 2015. Removing the "Plateau" from Hot White Dwarf Luminosity Functions. In: Dufour, P., Bergeron, P., Fontaine, G. (Eds.), 19th European Workshop on White Dwarfs. Vol. 493 of Astronomical Society of the Pacific Conference Series. p. 343.

Lamb, D. Q., van Horn, H. M., Sep. 1975. Evolution of crystallizing pure C-12 white dwarfs. ApJ 200, 306–323.

Lasserre, T., Afonso, C., Albert, J. N., Andersen, J., Ansari, R., Aubourg, É., Bareyre, P., Bauer, F., Beaulieu, J. P., Blanc, G., Bouquet, A., Char,

S., Charlot, X., Couchot, F., Coutures, C., Derue, F., Ferlet, R., Glicenstein, J. F., Goldman, B., Gould, A., Graff, D., Gros, M., Haissinski, J., Hamilton, J. C., Hardin, D., de Kat, J., Kim, A., Lesquoy, É., Loup, C., Magneville, C., Mansoux, B., Marquette, J. B., Maurice, É., Milsztajn, A., Moniez, M., Palanque-Delabrouille, N., Perdereau, O., Prévot, L., Regnault, N., Rich, J., Spiro, M., Vidal-Madjar, A., Vigroux, L., Zylberajch, S., EROS Collaboration, Mar. 2000. Not enough stellar mass Machos in the Galactic halo. A&A 355, L39–L42.

Leggett, S. K., Ruiz, M. T., Bergeron, P., Apr. 1998. The Cool White Dwarf Luminosity Function and the Age of the Galactic Disk. ApJ 497, 294–302.

Li, W., Van Dyk, S. D., Filippenko, A. V., Cuillandre, J.-C., Jha, S., Bloom, J. S., Riess, A. G., Livio, M., Apr. 2006. Identification of the Red Supergiant Progenitor of Supernova 2005cs: Do the Progenitors of Type II-P Supernovae Have Low Mass? ApJ 641, 1060–1070.

Liebert, J., 1979. The luminosity function and evolution of cool white dwarfs. In: van Horn, H. M., Weidemann, V. (Eds.), IAU Colloq. 53: White Dwarfs and Variable Degenerate Stars. pp. 146–164.

Liebert, J., Bergeron, P., Holberg, J. B., Jan. 2005. The Formation Rate and Mass and Luminosity Functions of DA White Dwarfs from the Palomar Green Survey. ApJS 156, 47–68.

Liebert, J., Dahn, C. C., Gresham, M., Strittmatter, P. A., Oct. 1979. New results from a survey of faint proper-motion stars - A probable deficiency of very low luminosity degenerates. ApJ 233, 226–238.

Liebert, J., Dahn, C. C., Monet, D. G., Sep. 1988. The luminosity function of white dwarfs. ApJ 332, 891–909.

Liebert, J., Dahn, C. C., Monet, D. G., 1989a. The luminosity function of white dwarfs in the local disk and halo. In: Wegner, G. (Ed.), IAU Colloq. 114: White Dwarfs. Vol. 328 of Lecture Notes in Physics, Berlin Springer Verlag. pp. 15–23.

Liebert, J., Dahn, C. C., Monet, D. G., 1989b. The luminosity function of white dwarfs in the local disk and halo. In: Wegner, G. (Ed.), IAU Colloq. 114: White Dwarfs. Vol. 328 of Lecture Notes in Physics, Berlin Springer Verlag. pp. 15–23.

Limoges, M.-M., Bergeron, P., May 2010. A Spectroscopic Analysis of White Dwarfs in the Kiso Survey. ApJ 714, 1037–1051.

Limoges, M.-M., Bergeron, P., Lépine, S., May 2015. Physical Properties of the Current Census of Northern White Dwarfs within 40 pc of the Sun. ArXiv e-prints.

Limoges, M.-M., Lépine, S., Bergeron, P., May 2013. Toward a Spectroscopic Census of White Dwarfs within 40 pc of the Sun. AJ 145, 136.

Lineweaver, C. H., May 1999. A Younger Age for the Universe. Science 284, 1503.

Lutz, T. E., Kelker, D. H., Oct. 1973. On the Use of Trigonometric Parallaxes for the Calibration of Luminosity Systems: Theory. PASP 85, 573.

Luyten, W., 1958. A search for faint blue stars: X. The Hyades: XI. The Pleiades. XIII. The region of Praesepe, XIV. The Ursa Major region. Publications of the Astronomical Observatory University of Minnesota, 1.

Luyten, W. J., 1922. The Mean Parallax of Early-Type Stars of Determined Proper Motion and Apparent Magnitude. PASP 34, 156.

Luyten, W. J., 1963. The motions of white dwarfs. Publications of the Astronomical Observatory University of Minnesota 17, 1.

Luyten, W. J., 1975. Luyten Half-Second (LHS) Catalog. University of Minnesota Press.

Lynden-Bell, D., 1971. A method of allowing for known observational selection in small samples applied to 3CR quasars. MNRAS 155, 95.

Majewski, S. R., Siegel, M. H., Apr. 2002. Absolute Proper Motions to B~22.5. IV. Faint, Low-Velocity White Dwarfs and the White Dwarf Population Density Law. ApJ 569, 432–445.

Marigo, P., Apr. 2001. Chemical yields from low- and intermediate-mass stars: Model predictions and basic observational constraints. A&A 370, 194–217.

Marigo, P., Girardi, L., Jul. 2007. Evolution of asymptotic giant branch stars. I. Updated synthetic TP-AGB models and their basic calibration. A&A 469, 239–263.

Maund, J. R., Smartt, S. J., Danziger, I. J., Nov. 2005. The progenitor of SN 2005cs in the Whirlpool Galaxy. MNRAS 364, L33–L37.

McCook, G. P., Sion, E. M., Mar. 1999. A Catalog of Spectroscopically Identified White Dwarfs. ApJS 121, 1–130.

Méndez, R. A., Minniti, D., Feb. 2000. Faint Blue Objects on the Hubble Deep Field North and South as Possible Nearby Old Halo White Dwarfs. ApJ 529, 911–916.

Méndez, R. A., Ruiz, M. T., Jan. 2001. The Luminosity Function of Magnitude and Proper-Motion-selected Samples: The Case of White Dwarfs. ApJ 547, 252–263.

Mestel, L., 1952. On the theory of white dwarf stars. I. The energy sources of white dwarfs. MNRAS 112, 583.

Mestel, L., Ruderman, M. A., 1967. The energy content of a white dwarf and its rate of cooling. MNRAS 136, 27.

Mihalas, D., Binney, J., 1981. Galactic astronomy: Structure and kinematics. W. H. Freeman and Co. (San Francisco, CA).

Miller Bertolami, M. M., Feb. 2014. Limits on the neutrino magnetic dipole moment from the luminosity function of hot white dwarfs. A&A 562, A123.

Miller Bertolami, M. M., Althaus, L. G., García-Berro, E., Sep. 2013. Quiescent Nuclear Burning in Low-metallicity White Dwarfs. ApJ 775, L22.

Miller Bertolami, M. M., Melendez, B. E., Althaus, L. G., Isern, J., Oct. 2014. Revisiting the axion bounds from the Galactic white dwarf luminosity function. J. Cosmol. & Astropart. Phys. 10, 69.

Mochkovitch, R., Jun. 1983. Freezing of a carbon-oxygen white dwarf. A&A 122, 212–218.

Mochkovitch, R., Garcia-Berro, E., Hernanz, M., Isern, J., Panis, J. F., Jul. 1990. Theoretical luminosity functions for halo white dwarfs. A&A 233, 456–461.

Monet, D. G., Fisher, M. D., Liebert, J., Canzian, B., Harris, H. C., Reid, I. N., Sep. 2000. A Survey for Faint Stars of Large Proper Motion Using Extra POSS II Plates. AJ 120, 1541–1547.

Montgomery, M. H., Klumpe, E. W., Winget, D. E., Wood, M. A., Nov. 1999. Evolutionary Calculations of Phase Separation in Crystallizing White Dwarf Stars. ApJ 525, 482–491.

Muraki, Y., Sumi, T., Abe, F., Bond, I., Carter, B., Dodd, R., Fujimoto, M., Hearnshaw, J., Honda, M., Jugaku, J., Kabe, S., Kato, Y., Kobayashi, M., Koribalski, B., Kilmartin, P., Masuda, K., Matsubara, Y., Nakamura, T., Noda, S., Pennycook, G., Rattenbury, N., Reid, M., Saito, T., Sato, H., Sato, S., Sekiguchi, M., Sullivan, D., Takeuti, M., Watase, Y., Yanagisawa, T., Yock, P., Yoshizawa, M., 1999. Search for Machos by the MOA Collaboration. Prog. of Theoretical Phys. Suppl. 133, 233–246.

Noh, H.-R., Scalo, J., Apr. 1990. History of the Milky Way star formation rate from the white dwarf luminosity function. ApJ 352, 605–614.

Oppenheimer, B. R., Hambly, N. C., Digby, A. P., Hodgkin, S. T., Saumon, D., Apr. 2001. Direct Detection of Galactic Halo Dark Matter. Science 292, 698–702.

Oswalt, T. D., Hintzen, P. M., Luyten, W. J., Apr. 1988. Identifications and limited spectroscopy for Luyten common proper motion stars with probable white dwarf components. I - Pair brighter than 17th magnitude. ApJS 66, 391–396.

Oswalt, T. D., Smith, J. A., Wood, M. A., Hintzen, P., Aug. 1996. A lower limit of 9.5 Gyr on the age of the Galactic disk from the oldest white dwarf stars. Nature 382, 692–694.

Panei, J. A., Althaus, L. G., Benvenuto, O. G., Mar. 2000. The evolution of iron-core white dwarfs. MNRAS 312, 531–539.

Pauli, E.-M., Napiwotzki, R., Altmann, M., Heber, U., Odenkirchen, M., Kerber, F., Mar. 2003. 3D kinematics of white dwarfs from the SPY project. A&A 400, 877–890.

Pauli, E.-M., Napiwotzki, R., Heber, U., Altmann, M., Odenkirchen, M., Feb. 2006. 3D kinematics of white dwarfs from the SPY project. II. A&A 447, 173–184.

Perryman, M. A. C., de Boer, K. S., Gilmore, G., Høg, E., Lattanzi, M. G., Lindegren, L., Luri, X., Mignard, F., Pace, O., de Zeeuw, P. T., Apr. 2001. GAIA: Composition, formation and evolution of the Galaxy. A&A 369, 339–363.

Pietrinferni, A., Cassisi, S., Salaris, M., Castelli, F., Sep. 2004. A Large Stellar Evolution Database for Population Synthesis Studies. I. Scaled Solar Models and Isochrones. ApJ 612, 168–190.

Prada Moroni, P. G., Straniero, O., Dec. 2002. Calibration of White Dwarf Cooling Sequences: Theoretical Uncertainty. ApJ 581, 585–597.

Prada Moroni, P. G., Straniero, O., May 2007. White dwarf cooling sequences. II. Luminosity functions. A&A 466, 1043–1051.

Rebassa-Mansergas, A., Liu, X.-W., Cojocaru, R., Yuan, H.-B., Torres, S., García-Berro, E., Xiang, M.-X., Huang, Y., Koester, D., Hou, Y., Li, G., Zhang, Y., Jun. 2015. DA white dwarfs from the LSS-GAC survey DR1: the preliminary luminosity and mass functions and formation rate. MNRAS 450, 743–762.

Reid, I. N., Sahu, K. C., Hawley, S. L., Oct. 2001. High-Velocity White Dwarfs: Thick Disk, Not Dark Matter. ApJ 559, 942–947.

Renedo, I., Althaus, L. G., Miller Bertolami, M. M., Romero, A. D., Córsico, A. H., Rohrmann, R. D., García-Berro, E., Jul. 2010. New Cooling Sequences for Old White Dwarfs. ApJ 717, 183–195.

Richer, H. B., Anderson, J., Brewer, J., Davis, S., Fahlman, G. G., Hansen, B. M. S., Hurley, J., Kalirai, J. S., King, I. R., Reitzel, D., Rich, R. M., Shara, M. M., Stetson, P. B., Aug. 2006. Probing the Faintest Stars in a Globular Star Cluster. Science 313, 936–940.

Richer, H. B., Fahlman, G. G., Rosvick, J., Ibata, R., Sep. 1998. The White Dwarf Cooling Age of M67. ApJ 504, L91–L94.

Richer, H. B., Hansen, B., Limongi, M., Chieffi, A., Straniero, O., Fahlman, G. G., Jan. 2000. Isochrones and Luminosity Functions for Old White Dwarfs. ApJ 529, 318–337.

Ritossa, C., García-Berro, E., Iben, Jr., I., Apr. 1999. On the Evolution of Stars that Form Electron-degenerate Cores Processed by Carbon Burning. V. Shell Convection Sustained by Helium Burning, Transient Neon Burning, Dredge-out, Urca Cooling, and Other Properties of an 11 M_{solar} Population I Model Star. ApJ 515, 381–397.

Rohrmann, R. D., May 2001. Hydrogen-model atmospheres for white dwarf stars. MNRAS 323, 699–712.

Rowell, N., Sep. 2013. The star formation history of the solar neighbourhood from the white dwarf luminosity function. MNRAS 434, 1549–1564.

Rowell, N., Hambly, N. C., Oct. 2011. White dwarfs in the SuperCOSMOS Sky Survey: the thin disc, thick disc and spheroid luminosity functions. MNRAS 417, 93–113.

Rubin, K. H. R., Williams, K. A., Bolte, M., Koester, D., Jun. 2008. The White Dwarf Population in NGC 1039 (M34) and the White Dwarf Initial-Final Mass Relation. AJ 135, 2163–2176.

Salaris, M., Althaus, L. G., García-Berro, E., Jul. 2013. Comparison of theoretical white dwarf cooling timescales. A&A 555, A96.

Salaris, M., Domínguez, I., García-Berro, E., Hernanz, M., Isern, J., Mochkovitch, R., Sep. 1997. The Cooling of CO White Dwarfs: Influence of the Internal Chemical Distribution. ApJ 486, 413–419.

Salaris, M., García-Berro, E., Hernanz, M., Isern, J., Saumon, D., Dec. 2000. The Ages of Very Cool Hydrogen-rich White Dwarfs. ApJ 544, 1036–1043.

Salaris, M., Serenelli, A., Weiss, A., Miller Bertolami, M., Feb. 2009. Semi-empirical White Dwarf Initial-Final Mass Relationships: A Thorough Analysis of Systematic Uncertainties Due to Stellar Evolution Models. ApJ 692, 1013–1032.

Salim, S., Gould, A., Aug. 2002. Classifying Luyten Stars Using an Optical-Infrared Reduced Proper-Motion Diagram. ApJ 575, L83–L86.

Salim, S., Gould, A., Jan. 2003. Improved Astrometry and Photometry for the Luyten Catalog. II. Faint Stars and the Revised Catalog. ApJ 582, 1011–1031.

Salpeter, E. E., Jan. 1955. The Luminosity Function and Stellar Evolution. ApJ 121, 161.

Salpeter, E. E., Nov. 1961. Energy and Pressure of a Zero-Temperature Plasma. ApJ 134, 669.

Sandage, A., Tammann, G. A., Yahil, A., Sep. 1979. The velocity field of bright nearby galaxies. I - The variation of mean absolute magnitude with redshift for galaxies in a magnitude-limited sample. ApJ 232, 352–364.

Sarna, M. J., Ergma, E., Gerškevitš-Antipova, J., Jul. 2000. Cooling curves and initial models for low-mass white dwarfs ($<0.25M_\odot$) with helium cores. MNRAS 316, 84–96.

Saumon, D., Jacobson, S. B., Feb. 1999. Pure Hydrogen Model Atmospheres for Very Cool White Dwarfs. ApJ 511, L107–L110.

Sayres, C., Subasavage, J. P., Bergeron, P., Dufour, P., Davenport, J. R. A., AlSayyad, Y., Tofflemire, B. M., Apr. 2012. A Multi-survey Approach to White Dwarf Discovery. AJ 143, 103.

Schmidt, M., Mar. 1959. The Rate of Star Formation. ApJ 129, 243.

Schmidt, M., Feb. 1968. Space Distribution and Luminosity Functions of Quasi-Stellar Radio Sources. ApJ 151, 393.

Schmidt, M., Nov. 1975a. The mass of the galactic halo derived from the luminosity function of high-velocity stars. ApJ 202, 22–29.

Schmidt, M., Nov. 1975b. The mass of the galactic halo derived from the luminosity function of high-velocity stars. ApJ 202, 22–29.

Segretain, L., Jun. 1996. Three-body crystallization diagrams and the cooling of white dwarfs. A&A 310, 485–488.

Segretain, L., Chabrier, G., Apr. 1993. Crystallization of binary ionic mixtures in dense stellar plasmas. A&A 271, L13.

Segretain, L., Chabrier, G., Hernanz, M., Garcia-Berro, E., Isern, J., Mochkovitch, R., Oct. 1994. Cooling theory of crystallized white dwarfs. ApJ 434, 641–651.

Serenelli, A. M., Althaus, L. G., Rohrmann, R. D., Benvenuto, O. G., Aug. 2001. The ages and colours of cool helium-core white dwarf stars. MNRAS 325, 607–616.

Serenelli, A. M., Althaus, L. G., Rohrmann, R. D., Benvenuto, O. G., Dec. 2002. Evolution and colours of helium-core white dwarf stars: the case of low-metallicity progenitors. MNRAS 337, 1091–1104.

Shaviv, G., Kovetz, A., Sep. 1976. The cooling of carbon-oxygen white dwarfs. A&A 51, 383–391.

Silvestri, N. M., Oswalt, T. D., Hawley, S. L., Aug. 2002. Wide Binary Systems and the Nature of High-Velocity White Dwarfs. AJ 124, 1118–1126.

Silvotti, R., Catalán, S., Cignoni, M., Alcalá, J. M., Capaccioli, M., Grado, A., Pannella, M., Apr. 2009. White dwarfs in the Capodimonte deep field. A&A 497, 109–116.

Sion, E. M., Greenstein, J. L., Landstreet, J. D., Liebert, J., Shipman, H. L., Wegner, G. A., Jun. 1983. A proposed new white dwarf spectral classification system. ApJ 269, 253–257.

Sion, E. M., Holberg, J. B., Oswalt, T. D., McCook, G. P., Wasatonic, R., Dec. 2009. The White Dwarfs Within 20 Parsecs of the Sun: Kinematics and Statistics. AJ 138, 1681–1689.

Sion, E. M., Holberg, J. B., Oswalt, T. D., McCook, G. P., Wasatonic, R., Myszka, J., Jun. 2014. The White Dwarfs within 25 pc of the Sun: Kinematics and Spectroscopic Subtypes. AJ 147, 129.

Sion, E. M., Liebert, J., Apr. 1977. The space motions and luminosity function of white dwarf. ApJ 213, 468–478.

Smartt, S. J., Maund, J. R., Hendry, M. A., Tout, C. A., Gilmore, G. F., Mattila, S., Benn, C. R., Jan. 2004. Detection of a Red Supergiant Progenitor Star of a Type II-Plateau Supernova. Science 303, 499–503.

Smith, J. A., 1997. White Dwarfs in Wide Binaries and the Age of the Galaxy. Ph.D. thesis, Florida Institute of Technology.

Smith, J. A., Oswalt, T. D., Wood, M. A., 2003. A Lower Limit to the Age of the Galaxy from the White Dwarf Luminosity Function. In: de Martino, D., Silvotti, R., Solheim, J.-E., Kalytis, R. (Eds.), NATO ASIB Proc. 105: White Dwarfs. p. 399.

Stevenson, D. J., Mar. 1980. A eutectic in carbon-oxygen white dwarfs. Journal de Physique 41, C61.

Subasavage, J. P., Henry, T. J., Hambly, N. C., Brown, M. A., Jao, W.-C., Finch, C. T., Oct. 2005. The Solar Neighborhood. XV. Discovery of New High Proper Motion Stars with $\mu \gtrsim 0.4''yr^{-1}$ between Declinations -47deg and 00deg. AJ 130, 1658–1679.

Suda, T., Komiya, Y., Yamada, S., Katsuta, Y., Aoki, W., Gil-Pons, P., Doherty, C. L., Campbell, S. W., Wood, P. R., Fujimoto, M. Y., May 2013. Transition of the stellar initial mass function explored using binary population synthesis. MNRAS 432, L46.

Tamanaha, C. M., Silk, J., Wood, M. A., Winget, D. E., Jul. 1990. The white dwarf luminosity function - A possible probe of the galactic halo. ApJ 358, 164–169.

Tisserand, P., Le Guillou, L., Afonso, C., Albert, J. N., Andersen, J., Ansari, R., Aubourg, É., Bareyre, P., Beaulieu, J. P., Charlot, X., Coutures, C., Ferlet, R., Fouqué, P., Glicenstein, J. F., Goldman, B., Gould, A., Graff, D., Gros, M., Haissinski, J., Hamadache, C., de Kat, J., Lasserre, T., Lesquoy, É., Loup, C., Magneville, C., Marquette, J. B., Maurice, É., Maury, A., Milsztajn, A., Moniez, M., Palanque-Delabrouille, N., Perdereau, O., Rahal, Y. R., Rich, J., Spiro, M., Vidal-Madjar, A., Vigroux, L., Zylberajch, S., EROS-2 Collaboration, Jul. 2007. Limits on the Macho content of the Galactic Halo from the EROS-2 Survey of the Magellanic Clouds. A&A 469, 387–404.

Torres, S., Camacho, J., Isern, J., García-Berro, E., Aug. 2008. The contribution of red dwarfs and white dwarfs to the halo dark matter. A&A 486, 427–435.

Torres, S., Camacho, J., Isern, J., García-Berro, E., Feb. 2010. White dwarfs with hydrogen-deficient atmospheres and the dark matter content of the Galaxy. A&A 511, A88.

Torres, S., García-Berro, E., Apr. 2016. The white dwarf population within 40 pc of the Sun. A&A 588, A35.

Torres, S., García-Berro, E., Burkert, A., Isern, J., Dec. 2001. The impact of a merger episode in the galactic disc white dwarf population. MNRAS 328, 492–500.

Torres, S., García-Berro, E., Burkert, A., Isern, J., Nov. 2002. High-proper-motion white dwarfs and halo dark matter. MNRAS 336, 971–978.

Torres, S., García-Berro, E., Isern, J., Nov. 1998. Neural Network Identification of Halo White Dwarfs. ApJ 508, L71–L74.

Torres, S., García-Berro, E., Isern, J., Jul. 2007. The white dwarf luminosity function - II. The effect of the measurement errors and other biases. MNRAS 378, 1461–1470.

Torres, S., García-Berro, E., Isern, J., Figueras, F., Jul. 2005. Simulating Gaia performances on white dwarfs. MNRAS 360, 1381–1392.

Torres, S., García-Berro, E., Krzesiński, J., Kleinman, S. J., Jan. 2013. Monte Carlo Simulations of the Luminosity Function of Hot White Dwarfs. In: Krzesiń, ski, J., Stachowski, G., Moskalik, P., Bajan, K. (Eds.), 18th European White Dwarf Workshop. Vol. 469 of Astronomical Society of the Pacific Conference Series. p. 109.

Torres, S., García-Berro, E., Krzesinski, J., Kleinman, S. J., Mar. 2014. A population synthesis study of the luminosity function of hot white dwarfs. A&A 563, A47.

Tremblay, P.-E., Kalirai, J. S., Soderblom, D. R., Cignoni, M., Cummings, J., Aug. 2014. White Dwarf Cosmochronology in the Solar Neighborhood. ApJ 791, 92.

Ubaldi, L., Jun. 2014. White dwarfs constraints on dark sector models with light particles. In: American Institute of Physics Conference Series. Vol. 1604 of American Institute of Physics Conference Series. pp. 128–133.

Udalski, A., Szymański, M., Stanek, K., Kaluny, J., Kubiak, M., Mateo, M., Krzeminski, B., Paczyński, B., R., V., Jan. 1996. The Optical Gravitational Lensing Experiment. The Optical Depth to Gravitational Microlensing in the Direction of the Galactic Bulge. Acta Astron. 44, 165–189.

Van Dyk, S. D., Li, W., Filippenko, A. V., Nov. 2003. On the Progenitor of the Type II-Plateau Supernova 2003gd in M74. PASP 115, 1289–1295.

van Horn, H. M., Jan. 1968. Crystallization of White Dwarfs. ApJ 151, 227.

Vennes, S., Kawka, A., Croom, S. M., Boyle, B. J., Smith, R. J., Shanks, T., Outram, P., Miller, L., Loaring, N., 2005. The white dwarf population in the 2QZ and SLOAN surveys. In: Sion, E. M., Vennes, S., Shipman, H. L. (Eds.), White dwarfs: cosmological and galactic probes. Vol. 332 of Astrophysics and Space Science Library. pp. 49–60.

Vila, S. C., May 1976. Changing gravitational constant and white dwarfs. ApJ 206, 213.

von Hippel, T., Apr. 1998. Contribution of White Dwarfs to Cluster Masses. AJ 115, 1536–1542.

von Hippel, T., Gilmore, G., Sep. 2000. The White Dwarf Cooling Age of the Open Cluster NGC 2420. AJ 120, 1384–1395.

von Hippel, T., Gilmore, G., Jones, D. H. P., Apr. 1995. An independent calibration of stellar ages: Hubble Space Telescope observations of white dwarfs at V=25. MNRAS 273, L39–L44.

Watson, A., Mar. 1998. Inflation Confronts an Open Universe. Science 279, 1455.

Wegner, G., 1973. A spectroscopic survey of southern hemisphere white dwarfs - III. Binaries containing a white dwarf. MNRAS 165, 271–294.

Wegner, G., Darling, G. W., 1994. White Dwarfs From the KISO Survey. In: Wallerstein, G., Noriega-Crespo, A. (Eds.), Stellar and Circumstellar

Astrophysics, a 70th birthday celebration for K. H. Bohm and E. Bohm-Vitense. Vol. 57 of Astronomical Society of the Pacific Conference Series. p. 178.

Weidemann, V., 1967. Leuchtkraftfunktion und räumliche Dichte der Weiβen Zwerge. Z. für Astr. 67, 286.

Weidemann, V., Aug. 1977. Mass loss towards the white dwarf stage. A&A 59, 411–418.

Weidemann, V., Dec. 1987. The initial-final mass relation - Galactic disk and Magellanic Clouds. A&A 188, 74–84.

Weidemann, V., Nov. 2000a. Revision of the initial-to-final mass relation. A&A 363, 647–656.

Weidemann, V., Nov. 2000b. Revision of the initial-to-final mass relation. A&A 363, 647–656.

Williams, K. A., Bolte, M., Koester, D., Mar. 2009. Probing the Lower Mass Limit for Supernova Progenitors and the High-Mass End of the Initial-Final Mass Relation from White Dwarfs in the Open Cluster M35 (NGC 2168). ApJ 693, 355–369.

Winget, D. E., Hansen, C. J., Liebert, J., van Horn, H. M., Fontaine, G., Nather, R. E., Kepler, S. O., Lamb, D. Q., Apr. 1987. An independent method for determining the age of the universe. ApJ 315, L77–L81.

Winget, D. E., Sullivan, D. J., Metcalfe, T. S., Kawaler, S. D., Montgomery, M. H., Feb. 2004. A Strong Test of Electroweak Theory Using Pulsating DB White Dwarf Stars as Plasmon Neutrino Detectors. ApJ 602, L109–L112.

Wood, M. A., Feb. 1992. Constraints on the age and evolution of the Galaxy from the white dwarf luminosity function. ApJ 386, 539–561.

Wood, M. A., 1995. Theoretical White Dwarf Luminosity Functions: DA Models. In: Koester, D., Werner, K. (Eds.), White Dwarfs. Vol. 443 of Lecture Notes in Physics, Berlin Springer Verlag. p. 41.

Wood, M. A., Oswalt, T. D., Apr. 1998. White Dwarf Cosmochronometry. I. Monte Carlo Simulations of Proper-Motion- and Magnitude-Limited Samples using Schmidt's $1/V_{max}$ Estimator. ApJ 497, 870–882.

Xu, Z. W., van Horn, H. M., Mar. 1992. Effects of Fe/C phase separation on the ages of white dwarfs. ApJ 387, 662–672.

Yoo, J., Chanamé, J., Gould, A., Jan. 2004. The End of the MACHO Era: Limits on Halo Dark Matter from Stellar Halo Wide Binaries. ApJ 601, 311–318.

Yuan, J. W., Oct. 1989. White dwarf luminosity functions calculated from models of galactic evolution and the age of the galactic disk. A&A 224, 108–116.

Zhao, J. K., Oswalt, T. D., Willson, L. A., Wang, Q., Zhao, G., Feb. 2012. The Initial-Final Mass Relation among White Dwarfs in Wide Binaries. ApJ 746, 144.